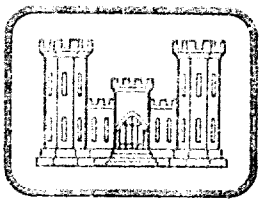

LEVEL II

TECHNICAL REPORT EL-81-2

THERMAL MODELING OF TERRAIN SURFACE ELEMENTS

by

L. K. Balick, L. E. Link, R. K. Scoggins

Environmental Laboratory
U. S. Army Engineer Waterways Experiment Station
P. O. Box 631, Vicksburg, Miss. 39180

and

J. L. Solomon

Department of Mathematics
Mississippi State University
Starkville, Miss. 39762

March 1981

Final Report

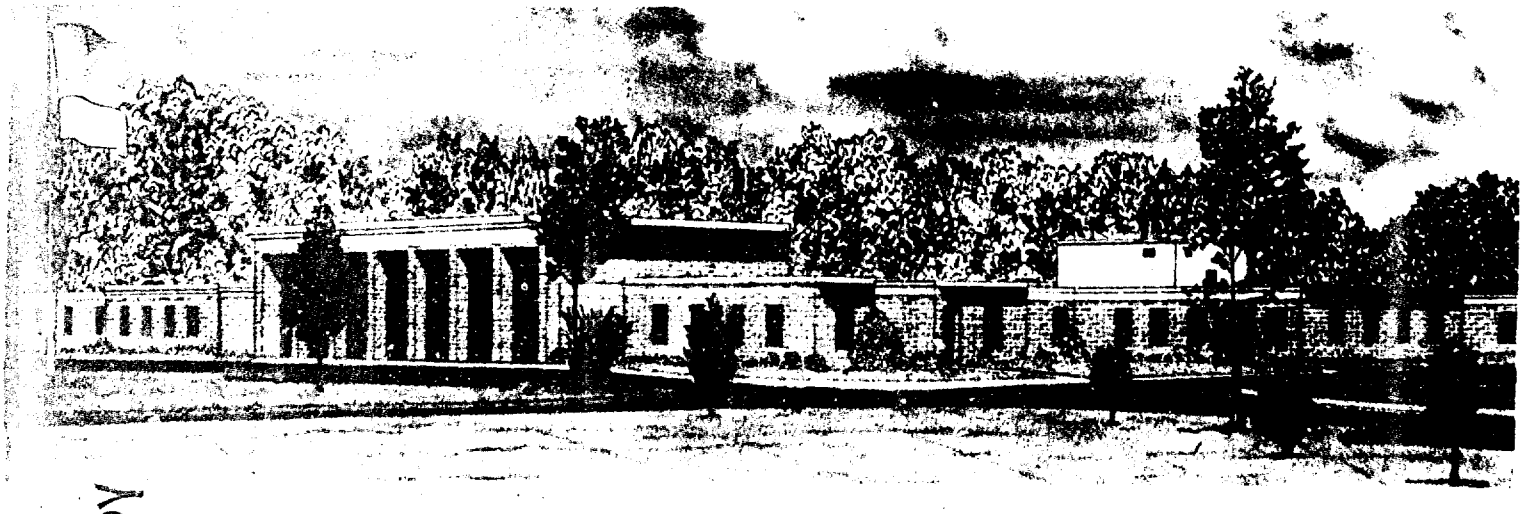

Prepared for Headquarters, Department of the Army
Washington, D. C. 20314

Under Project 4762730AT42, Task A4, Work Unit 003 and
4762719AT40, Task CO, Work Unit 006

Destroy this report when no longer needed. Do not return it to the originator.

The findings in this report are not to be construed as an official Department of the Army position unless so designated by other authorized documents.

The contents of this report are not to be used for advertising, publication, or promotional purposes. Citation of trade names does not constitute an official endorsement or approval of the use of such commercial products.

Unclassified

SECURITY CLASSIFICATION OF THIS PAGE (When Data Entered)

(14) WES/TR/EL-81-2

REPORT DOCUMENTATION PAGE

READ INSTRUCTIONS BEFORE COMPLETING FORM

1. REPORT NUMBER: Technical Report EL-81-2
2. GOVT ACCESSION NO.: AD-A098 019
3. RECIPIENT'S CATALOG NUMBER: (9)

4. TITLE (and Subtitle): (6) THERMAL MODELING OF TERRAIN SURFACE ELEMENTS.
5. TYPE OF REPORT & PERIOD COVERED: Final report, 1 Oct 78 — 1 Jun 80
6. PERFORMING ORG. REPORT NUMBER:

7. AUTHOR(s): (10) L. K. Balick, L. E. Link, R. K. Scoggins, J. L. Solomon
8. CONTRACT OR GRANT NUMBER(s): 4A762730AT42, 4A762719AT40

9. PERFORMING ORGANIZATION NAME AND ADDRESS: Department of Mathematics, Mississippi State University, Starkville, Miss. 39762 and (17) AT, CO Environmental Laboratory, U. S. Army Engineer Waterways Experiment Station, P. O. Box 631, Vicksburg, Miss. 39180
10. PROGRAM ELEMENT, PROJECT, TASK AREA & WORK UNIT NUMBERS: Project No. 4762730AT42, Task A4, Work Unit 003; and 4A762719AT40, Task CO, Work Unit 006

11. CONTROLLING OFFICE NAME AND ADDRESS: Headquarters, Department of the Army, Washington, D. C. 20314
12. REPORT DATE: (11) Mar 81
13. NUMBER OF PAGES: 84 (12) 70
14. MONITORING AGENCY NAME & ADDRESS (if different from Controlling Office)
15. SECURITY CLASS. (of this report): Unclassified
15a. DECLASSIFICATION/DOWNGRADING SCHEDULE

16. DISTRIBUTION STATEMENT (of this Report): (20) L. K. Balick, L. E. Link, R. K. Scoggins, J. L. Solomon

Approved for public release; distribution unlimited.

17. DISTRIBUTION STATEMENT (of the abstract entered in Block 20, if different from Report)

18. SUPPLEMENTARY NOTES

19. KEY WORDS (Continue on reverse side if necessary and identify by block number)

Infrared detectors	Terrain models (Analytical)
Mathematical models	Terrain Surface Temperature Model
Target recognition	Thermal analysis
Temperature	

20. ABSTRACT (Continue on reverse side if necessary and identify by block number)

Historically, surveillance and target acquisition devices have operated in the visible portion of the spectrum where the eye was the dominant sensor. The eye is still a critical component in a surveillance or target acquisition system; however, the eye may now be aided by an infrared (IR) detection and image display capability. Also, weapons systems have IR seekers, sensor devices that allow the weapon to detect and lock on to a target that has a thermal

(Continued)

DD FORM 1 JAN 73 1473 EDITION OF 1 NOV 65 IS OBSOLETE

Unclassified

SECURITY CLASSIFICATION OF THIS PAGE (When Data Entered)

41 328

20. ABSTRACT (Continued).

signature significantly different from its surround. The thrust in the United States to further develop IR target acquisition and surveillance capabilities and the thrust in the North Atlantic Treaty Organization (NATO) community to camouflage or conceal critical elements at fixed installations from such devices have focused attention on the need to better understand the character of the thermal IR signatures of not only targets but also their surrounds. To date, considerably more effort has been focused on targets than or surrounds.

The Terrain Surface Temperature Model (TSTM) presented herein, was developed to help fill the void in the understanding of thermal IR signatures of natural terrain surfaces and of some cultural features. The model estimates temperatures of actual or hypothetical material systems and for actual or hypothetical weather conditions. The model handles sensible heat transfer, latent heat transfer, the impact of cloud type and cover, and seasonal/ geothermal heat fluxes. The material system can be handled as a multilayered medium with discrete physical and thermal properties assigned to each layer.

This report documents the TSTM by presenting a discussion of the mathematics of the model, a discussion of the computer program input file and its operation, and the results of a sensitivity analyses and limited verification tests conducted with the model. Typical parameter values of material systems descriptors used in the model are included in an appendix.

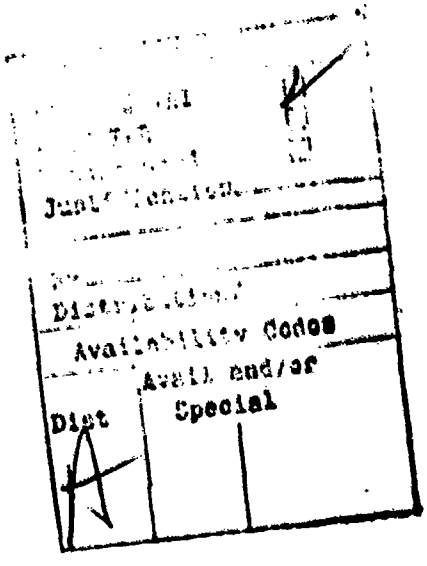

PREFACE

The study reported herein was conducted by personnel of the U. S. Army Engineer Waterways Experiment Station (WES) from 1 Oct 1978 to 1 Jun 1980. The study was done under Department of the Army Project No. 4A762730AT42, Task A4, Terrain/Operations Simulation, Work Unit 003, Electromagnetic Target Surround Characteristics in Natural Terrains, and Department of the Army Project No. 4A762719AT40, Task CO, Theater of Operations Construction, Work Unit 006, Fixed Installation Camouflage Methods and Materials.

The study was conducted under the general supervision of Dr. John Harrison, Chief of the Environmental Laboratory (EL), and Mr. Bob Benn, Chief of the Environmental Systems Division (ESD), EL, and under the direct supervision of Dr. Lewis E. Link, Jr., Chief of the Environmental Constraints Group (ECG), EL. The development of the mathematical model presented herein was accomplished primarily by Dr. Lee Balick, on assignment to ECG from Colorado State University. Assistance was received from Messrs. Randy Scoggins and Curt Gladen, ECG, and Dr. James Solomon, Mississippi State University, through an Army Research Office/Battelle Institute grant for temporary assistance. This report was prepared primarily by Dr. Balick with assistance from Dr. Link, Mr. Scoggins, and Dr. Solomon.

Directors of the WES during the conduct of the study were COL John L. Cannon, CE, and COL Nelson P. Conover, CE. Technical Director was Mr. Fred R. Brown.

This report should be cited as follows:

> Balick, L. K., Link, L. E., Scoggins, R. K., and Solomon, J. L. 1981. "Thermal Modeling of Terrain Surface Elements," Technical Report EL-81-2, prepared by the Environmental Laboratory, Waterways Experiment Station, in collaboration with Mississipi State University, for the U. S. Army Engineer Waterways Experiment Station, CE, Vicksburg, Miss.

CONTENTS

CONVERSION FACTORS, U. S. CUSTOMARY TO METRIC (SI) UNITS OF MEASUREMENT

U. S. customary units of measurement used in this report can be converted to metric (SI) units as follows:

Multiply	By	To Obtain
British thermal units (International Table)	1055.056	joules
degrees (angle)	0.01745329	radians
feet	0.3048	metres

THERMAL MODELING OF TERRAIN SURFACE ELEMENTS

PART I: INTRODUCTION

Background

1. Camouflage and target acquisition have opposing functions, one to hide and the other to seek. They have a common denominator, however, in that the features that surround the target to be camouflaged or identified (sometimes called the background) are critical in both the hide and seek role. An equally intimate knowledge is needed of the characteristics of both the target and the background. In essence, making something match the background and discriminating something from the background are inverse problems that require the same technology.

2. Historically, surveillance and target acquisition devices have operated in the visual wavelength bands where the eye remains a dominant sensor. In the past decade, thermal infrared (IR) technology has come of age providing sensors with new capabilities for target acquisition and presenting a new threat for camouflage. Optimizing IR sensors for target acquisition or optimizing camouflage measures to defeat such sensors requires a quantitative understanding of the thermal IR signatures of both targets and backgrounds. Because of the large impact of such factors as air temperature, solar insolation, wind, and cloud conditions thermal signatures can vary rapidly--an additional complication for consistent performance of either target acquisition sensors or camouflage measures.

3. The Army-Wide Ground Target Signature Program (AWGTSP) is addressing the need for a target-background design data base for sensor design and evaluation through a three-part program. The first part deals with the development of a battlefield IR signature model that will allow extrapolations of target and background signatures to varying environmental, climatic, and seasonal conditions throughout the world. The second area deals with updating a tactical signature library to fill

critical gaps in the existing empirical signature data base. The third program area deals with susceptibility analyses and is designed to ensure that vulnerability of all Army tactical materiel is known so that effective camouflage can be brought to bear.

4. An equally important problem is the camouflage of key elements at fixed installations, a responsibility of the U. S. Army Corps of Engineers, for which similar background and target information is needed. These objectives cannot be achieved solely on the basis of measured signature data or performance tests in the field. Modeling and simulation offer the tissue to tie measured data together and allow extrapolations to other environmental conditions, sensor types, and camouflage materials.

5. Work on the AWGTSP has resulted in considerable progress in computer codes for predicting the performance of surveillance, target acquisition, and terminal homing devices and target signatures. The target models have ranged from simple to complex, the more sophisticated approaches using combinatorial geometry. To date, targets have received considerably more attention than backgrounds. Since both the target and target surround have to be dealt with simultaneously in a battlefield scenario, a compatible and equally capable target-surround modeling procedure is needed.

6. A previous U. S. Army Engineer Waterways Experiment Station (WES) study (Link 1979) defined a research approach for developing a realistic target-surround signature data base for use in the design and evaluation of imaging and nonimaging sensors for surveillance, target acquisition, and terminal homing devices, and presented preliminary procedures for predicting terrain surface temperatures of typical components of battlefield environmental settings with special emphasis on the Federal Republic of Germany (GE). The work consisted of formulating terrain and climatic data bases for the GE, assembling computer models for predicting the diurnal temperatures of broad classes of terrain components as a function of climatic conditions, and developing a matrix for integrating the GE data bases and the temperature models to provide the initial capability to predict expected temperature ranges for terrain surface features under a variety of battlefield scenarios.

7. The work accomplished in the above referenced study provided an initial framework, however cursory, for estimating thermal regimes of terrain surface features for specific climatic conditions. Although the data base-model framework is valid, many gaps, both data and analytical, were evident. These gaps and the perceived capabilities needed to allow complete appraisal of the performance of electro-optical systems have been the focus of additional research.

8. The work that followed focused primarily on an enhancement of the mathematical modeling capabilities illustrated in the referenced report. As in the previous study, the modeling efforts were separated into two thrusts--models for vegetation canopies and models for nonvegetative surfaces such as soil, rock, and roadways. The vegetation canopy modeling has been accomplished primarily by Colorado State University (CSU) (Smith et al. 1980) under contract to the WES. The Thermal Vegetation Canopy Model developed by CSU is described in the reference cited. The terrain surface (nonvegetative) thermal modeling work was done primarily inhouse at the WES and is the subject of this report.

Objective and Scope

Objective

9. The objective of the work presented herein was to generate a capability to realistically predict the temperature (and radiative signature) histories of nonvegetative natural and cultural features that commonly comprise the backgrounds to targets. The ability to project background temperatures/signatures provides a means to examine temperature/signature contrasts that occur between targets and background features both with time and changing weather conditions. This in turn provides the basic information needed to examine the performance of existing or proposed target acquisition devices and the effectiveness of alternative camouflage measures.

Terrain Surface Temperature Model

10. The Terrain Surface Temperature Model (TSTM) was developed

to estimate the temperatures of actual or hypothetical material systems and for actual or hypothetical weather conditions. A premium was placed on simplicity and flexibility with respect to operational constraints. In short, a model was needed that considered the dominant physical phenomena that influence material temperatures and yet was reasonable to use. Some of the characteristics of the model developed to meet these requirements are as follows:

a. Time dependence through one diurnal cycle.

b. Air temperature as a state variable.

c. A system described with up to six layers of uniform properties.

d. Precipitation and condensation not considered.

e. Spectral characteristics of materials not considered.

The model handles sensible heat transfer, latent heat transfer, the impact of cloud type and cover, and seasonal/geothermal heat fluxes.

Scope of report

11. The TSTM is documented in this report. The documentation is comprised of a discussion of the mathematical model (Part II), a discussion of the computer program input description and its operation (Part III), and presentation of the results of a sensitivity analysis and limited verification tests conducted with the model (Part IV). In Part II, the mathematical framework of the model and associated assumptions are presented, followed by discussions of the surface and bottom boundary conditions considered and the mathematics used to describe relevant phenomena. The numerical techniques used to solve the heat transfer equation are then presented.

12. In Part III, considerations are given for selecting descriptors of material systems and atmospheric conditions as well as selecting options for computer code operation. These considerations are organized according to the major types of inputs to the computer code since virtually all material system and atmospheric condition discriptors and control messages for program options are included in the input data file. The sensitivity analysis in Part IV is subdivided into discussions on atmospheric parameters, material system parameters, and control

parameters for the numerical solution technique. Model verification tests were conducted by comparing model predicted surface temperature values to measurements of bare soil and concrete surface temperature. Part V presents conclusions and recommendations.

13. Two appendices are provided. Appendix A presents a simplified flow chart for the computer code, and Appendix B gives typical values for many of the material system descriptors used in the model.

PART II: MATHEMATICAL MODEL

Introduction

14. A general schematic of the TSTM concept is shown in Figure 1. The model predicts surface temperatures for a multilayered (1-6 layers) system by determining energy transfer in, out, and through the system. A basic assumption in the model is that the layers and the environment above them are horizontally uniform; i.e., the most significant heat fluxes are vertical. Thus the temperature T estimates result from solving the one-dimensional heat equation

$$\frac{\partial T(z,t)}{\partial t} = \alpha(z) \frac{\partial^2 T(z,t)}{\partial z^2}$$

subject to the boundary conditions

$$\sum_{i=1}^{n} b_{it} = 0 \quad \text{at} \quad z = 0$$

and

$$\sum_{i=1}^{n} B_{it} = 0 \quad \text{at} \quad z = b$$

where the observable surface is $z = b$, lower surface is $z = B$, $\alpha(z)$ is the diffusivity and both b_{it} and B_{it}, $i = 1,2,\ldots,n$, denote heat fluxes at time t.

15. Reliability of the results depends upon the extent to which the thermal characteristics in each of the layers can be approximated by constant values and also is strongly dependent upon the approximations of b_{it}, $i = 1,2,\ldots,n$, taking place at the surface which is exposed to environmental heat fluxes.

Surface Boundary Conditions

16. The boundary condition at the surface is estimated with a

heat balance equation composed of six energy components: (a) insolation; (b) radiant energy from the atmosphere and clouds; (c) radiant energy emitted by the top surface; (d) sensible heat loss (conduction and convection); (e) latent heat loss (evaporation); and (f) heat conduction into the material. A value for each of these components is calculated at each time increment.

Solar energy input

17. The main energy input to the surface boundary is insolation. The model allows the option for measured values to be input into the program or (by default) the values can be estimated by a series of empirical relations. Adjustments to measured data to account for differences of surface slope and cloud conditions must be made external to the program.

18. If the option of having the model estimate insolation values is chosen, a series of calculations is executed. All solar radiation is considered to be direct; i.e., if it is found that the sun is not shining directly upon the surface, then it is assumed that there is no solar radiation. If there is direct radiation, the radiation is modified to include the effects of: (a) attenuation due to atmospheric gases and water vapor; (b) attenuation due to cloud cover; (c) orientation of the surface to the sun; and (d) reflection at the surface.

19. In order to determine whether direct solar radiation occurs, the sun's position relative to the plane of the surface is computed. If there is no insolation at the surface, the calculation stops here. The equations for sun-slope geometry for a horizontal surface are those of Small (1977) and those of Sellers (1965) for sloped surfaces. Chapter 3 of Sellers (1965) has an excellent discussion of sun-slope geometry calculations.

20. The following equation is taken from Khale (1977) and is used to compute insolation:

$$S_a = (1 - \alpha_g)[1 - A(u^*,z)](0.349)S_o \cos z$$

$$+ (1 - \alpha_g)[(1 - \alpha_o)/(1 - \alpha_o\bar{\alpha}_g)](0.651)S_o \cos z$$

where

S_a = the solar radiation absorbed at the ground with no cloud cover

α_g = surface albedo

$A(u^*,z)$ = Mugge-Möller absorption function, equal to $0.271(u^* \sec z)^{0.803}$

u^* = effective water vapor content of atmosphere

$(0.349)S_o$ = amount of solar radiation of wavelength greater than 0.9 μm

S_o = solar radiation incident on top of the atmosphere

z = zenith angle of the sun as a function of time of the day and time of the year

α_o = atmospheric albedo for Rayleigh scattering, equal to $0.085 - 0.247 \log_{10} [(\rho_s/\rho_o) \cos z]$

ρ_s = surface pressure

ρ_o = 1000 mb

$\underline{\alpha}_g$ = area average ground albedo

$(0.651)S_o$ = amount of solar radiation of wavelength less than 0.9 μm

Excluding clouds, the effective water vapor content, u^*, is the total precipitable water in units of grams per square centimetre. Precipitable water is estimated from surface air temperature and relative humidity with the following equation (Smith 1966):

$$u^* = \exp [0.07074\ T_d + \tau]$$

where T_d is the dew point temperature (degrees Celsius) and $\tau = -0.02290$ from April to June and $\tau = 0.02023$ in other months.

21. Haurwitz's (1948) empirical equation is employed for overcast sky adjustments with respect to cloud cover and type:

$$CA = (a/94.4) \times \exp [-m \times (b - 0.059)]$$

where CA is the cloud adjustment factor, a and b are empirical coefficients dependent upon cloud type, and m is the secant of the

solar zenith angle. Values for a and b are available for the following eight cloud genera: cirrus, cirrostratus, altocumulus, altostratus, stratocumulus, stratus, nimbostratus, and fog (Table 1). Following work by Pochop, Shanklin, and Horner (1968), which suggests interpolation by the square of the cloud cover, the model employs the following interpolatory equation for intermediate cloud cover situations:

$$S_c = S_a - \left\{[S_a - (S_a \times CA)] \times CC^2\right\}$$

where S_c is the energy reaching the upper surface and CC is the visual cloud cover in tenths.

22. After the influence of clouds is estimated, the net insolation (S_b) is adjusted to account for the surface slope orientation to compute effective incident net insolation, S , as follows:

$$S = S_c \times SF$$

The slope factor (SF) is defined by:

$$SF = \cos(z)\cos(Sl) + \sin(z)\sin(Sl)\cos(SAZ - SlAZ)$$

where z is the solar zenith angle, Sl is the slope of the surface (angle between slope and horizontal), SAZ is the solar azimuth angle and SlAZ is the azimuth of the slope. (Azimuths are measured from the south, negatively increasing from south to east and positively increasing from south to west.)

Atmospheric and cloud
thermal IR energy inputs

23. The empirical equation used to estimate atmospheric IR radiation on the surface $I\downarrow_o$ is the Brunt equation (Sellers 1965):

$$I\downarrow_o = \varepsilon\sigma T_a^4 \left[c + b\left(e_a^{0.5}\right)\right]$$

where ε is the emissivity and assumed to be equal to 1, σ is the

Stephan-Boltzman constant, T_a is the shelter air temperature (degrees Kelvin), e_a is the water vapor pressure (millibars) and b and c are empirical constants. The values of Budyko as referenced by Sellers (1965) are used; i.e., $c = 0.61$ and $b = 0.050$. The value of e_a is obtained from Teten's equation (Murry 1967)

$$e_a = RH \times 6.108 \times \exp (A \times T_a)/(T_a + 273.15 - B)$$

where RH is the decimal relative humidity, $A = 17.269$ and $B = 35.86$. The cloud contributions to thermal IR irradiance $I\downarrow_t$ are treated with an empirical factor adapted from Sellers (1965):

$$I\downarrow_t = I\downarrow_o \times (1 + CIR \times CC^2)$$

where CIR is a coefficient dependent upon cloud type. Values for CIR can be found in Sellers (1965) or Oke (1978).

Ground radiative emittance

24. The surface is treated as a grey body emitter such that

$$I\uparrow = \varepsilon_g \sigma (T_g)^4$$

where $I\uparrow$ is the energy radiated from the surface, ε_g is the emissivity of the ground, and T_g is the current surface temperature as predicted by the model.

Sensible heat

25. The conductive and convective sensible heat transfer H is estimated by an equation following Lamb (1974) or Oke (1978).

$$H = -\rho C_p \kappa^2 z^2 \frac{\partial \theta}{\partial z} \frac{\partial v}{\partial z} SCF$$

where

$$SCF = \begin{cases} 1.175(1 - 15Ri)^{0.75} & Ri \leq 0 \\ (1 - 5Ri)^2 & 0 < Ri \leq 0.2 \\ 0 & Ri > 0.2 \end{cases}$$

and ρ is the air density, C_p is the specific heat of dry air at constant pressure, κ is von Karman's constant (0.40), z is the observation height, $\partial\theta/\partial z$ and $\partial v/\partial z$ are the partial derivatives of potential temperature and wind speed, respectively, with respect to height z. Ri denotes the Richardson number. Potential temperature θ is defined by the relation

$$\theta = T_a\left(\frac{1000}{p}\right)^{0.286}$$

where T_a and p are the air temperature and pressure, respectively. The Richardson number is defined by:

$$Ri = \left(\frac{g}{\theta}\frac{\partial\theta}{\partial z}\right)\Big/\left(\frac{\partial v}{\partial z}\right)^2$$

where g is the acceleration due to gravity and $\bar{\theta}$ is the average potential temperature between the surface and height z. In the model, $\partial\theta/\partial z$ and $\partial v/\partial z$ are approximated by first order differences, and it is assumed that the air temperature at the surface equals the surface temperature and that the wind velocity is zero at the surface. Although these assumptions at the surface are questionable, they eliminate the need for and difficulties in determining aerodynamical characteristics of the surface. This formulation was selected after discussions with Holbo.* The validity of the assumptions at the surface is doubtful, but they seem preferable to the selection of aerodynamic characteristics (like roughness) and attendant assumptions when a wide and unpredictable variety of surfaces are to be modeled.

Latent heat

26. The following equation (Oke 1978, Lamb 1974) for latent heat exchange E is used:

$$E = -\rho L\kappa^2 z^2 (W\partial q/\partial z)(\partial v/\partial z)SCF$$

---

* Personal communication, R. Holbo, Forest Research Laboratory, Oregon State University, Corvallis, Oreg.

where SCF is defined above, L is the latent heat of evaporation (Hess 1959), q is the specific humidity, and W is the decimal relative saturation of the top surface. In calculating a value for $\partial q/\partial z$, the air at the ground is assumed saturated. The value of q at $z = Z$ represents air at the instrument shelter; i.e., $\partial q/\partial z$ represents the potential gradient over a saturated surface. It is modified by the saturation factor W to account for nonsaturated conditions. As with the sensible heat loss calculation, E is set equal to zero if the air temperature at the surface is less than or equal to the air temperature at the shelter height.

Bottom Boundary Condition

27. The bottom boundary condition is the heat flux through the bottom of the lowest layer (top layer is numbered 1, second layer is 2, etc. to the last layer (maximum of 6)). The bottom boundary condition is specified by one of the following three options:

a. Option 1. A constant temperature at the bottom boundary.

b. Option 2. A constant heat flux at the bottom boundary.

c. Option 3. A constant heat flux at the bottom boundary and an additional constant temperature radiating surface below the bottom boundary.

28. The third option requires additional input: (a) bottom boundary thermal IR emissivity; (b) bottom boundary geometric shape factor; (c) under surface thermal IR emissivity; (d) under surface geometric shape factor; and (e) under surface temperature. Geometric shape factors vary from 0.0 to 1.0 and are related to the emitting and adsorbing "efficiency" of the surface. High efficiencies result from black flat surfaces of large horizontal dimensions. Deviations from this configuration suggest lower values but, unfortunately, there is little basis for selecting values less than 1.0. Regardless of the option chosen, the bottom boundary condition is kept constant in time.

Numerical Solution

29. The complicated nonlinear boundary conditions require that the heat conduction equation

$$\frac{\partial T(z,t)}{\partial t} = \alpha(z) \frac{\partial^2 T(z,t)}{\partial z^2}$$

be solved numerically. In this equation, α is the diffusivity. Each layer is assumed to be homogeneous, and it is assumed that the thermal characteristics can be taken to be constant; specifically, the thermal conductivity and diffusivity for each layer are assumed to be a constant.

Solution within a layer

30. Within each layer, an explicit scheme is employed to solve the one-dimensional heat equation. In particular, given the temperature profile at time t, the temperature at time $t + \Delta t$ at the node z is given by

$$T(t + \Delta t, z) = T(t,z) + \alpha(\Delta t/\Delta z^2)[T(t, z + \Delta z) - 2T(t,z) + T(t, z - \Delta z)]$$

where Δt is the time increment and Δz denotes the spatial increment. It should be noted that numerical stability requires $\alpha \Delta t/\Delta z^2 < 1/2$. The problem of numerical stability is critical for thin highly conductive layers.

Solution at the interface of two layers

31. The following derivation of an explicit finite difference scheme to handle the interface between layers is a modification of that presented in Carnahan, Luther, and Wilkes (1964). The derivation assumes perfect thermal contact at the interface, i.e., continuity of the heat flux and temperatures at the interfaces.

32. Let layer 1 have thermal conductivity k_1 and diffusivity α_1 and layer 2 have thermal conductivity and diffusivity k_2 and α_2, respectively.

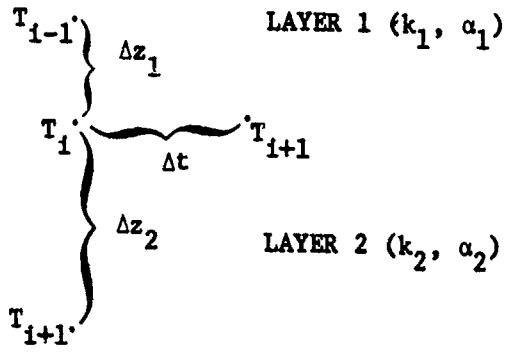

33. Knowing the temperature T_{i-1}, T_i, and T_{i+1} at the node points $i - 1$, i, and $i + 1$, the problem is to calculate the new temperature T_i' at the interface. Employing the truncated Taylor series, T_{i-1} is approximated by

$$T_{i-1} = T_i - \Delta z_1 \left(\frac{\partial T}{\partial z}\right)_{i1} + \frac{\Delta z_1^2}{2}\left(\frac{\partial^2 T}{\partial z^2}\right)_{i1}$$

where $i1$ denotes the partial derivative in layer 1 at the interface. Thus,

$$\left(\frac{\partial^2 T}{\partial z^2}\right)_{i1} = \frac{2}{\Delta z_1^2}\left[T_{i-1} - T_i + \Delta z_1 \left(\frac{\partial T}{\partial z}\right)_{i1}\right]$$

Also, the first order approximation to $\partial T/\partial t$ is given by

$$\left(\frac{\partial T}{\partial t}\right)_{i1} = \frac{T_i' - T_i}{\Delta t}$$

Since $\partial T/\partial t = \alpha_1(\partial^2 T/\partial z^2)$, one obtains

$$\frac{T_i' - T_i}{\Delta t} = \frac{2\alpha_1}{\Delta z_1^2}\left[T_{i-1} - T_1 + \Delta z_1 \left(\frac{\partial T}{\partial z}\right)_{i1}\right]$$

or

$$\frac{k_1 \Delta z_1^2}{2\alpha_1 \Delta z_1}\left[\frac{T_i' - T_i}{\Delta t}\right] - k_1 \frac{T_{i-1}}{\Delta z_1} + \frac{k_1 T_i}{\Delta z_1} = k_1 \left(\frac{\partial T}{\partial z}\right)_{i1}$$

i.e.,

$$k_1 \left(\frac{\partial T}{\partial z}\right)_{i1} = \frac{k_1}{2\Delta z_1 \alpha_1 \left(\Delta t/\Delta z_1^2\right)} [T_i' - T_i] - \frac{k_1}{\Delta z_1} T_{i-1} + \frac{k_1 T_1}{\Delta z_1} \qquad (1)$$

34. In a similar fashion for layer 2, one obtains

$$k_2 \left(\frac{\partial T}{\partial z}\right)_{i2} = \frac{-k_2}{2\Delta z_2 \alpha_2 \left(\Delta t/\Delta z_2^2\right)} [T_i' - T_i] + \frac{k_2 T_{i+1}}{\Delta z_2} - \frac{k_2 T_i}{\Delta z_2} \qquad (2)$$

Continuity of the heat flux implies that Equation 1 equals Equation 2; thus, after simplification, the final equation used to calculate T_i' is:

$$\left[\frac{k_1}{2\Delta z_1 \alpha_1 \left(\Delta t/\Delta z_1^2\right)} + \frac{k_2}{2\Delta z_2 \alpha_2 \left(\Delta t/\Delta z_2^2\right)}\right] T_i' = \left[\frac{k_1}{2\Delta z_1 \alpha_1 \left(\Delta t/\Delta z_1^2\right)}\right.$$

$$\left. + \frac{k_2}{2\Delta z_2 \alpha_2 \left(\Delta t/\Delta z_2^2\right)}\right] T_i + \frac{k_1}{\Delta z_1} T_{i-1} - \left(\frac{k_1}{\Delta z_1} + \frac{k_2}{\Delta z_2}\right) T_i + \frac{k_2}{\Delta z_2} T_{i+1}$$

Upper boundary

35. The new or updated value of the surface temperature $T(t + \Delta t, 0)$ is calculated by solving the surface heat balance equation for the surface temperature T_g. The heat balance equation is

$$S + I\downarrow_t - H - E - I\uparrow + G = 0 \qquad (3)$$

where G denotes the heat flux into the surface; i.e., $G = k(\partial T/\partial z)$ and is approximated by $k(T_1 - T_g/\Delta z)$ where k denotes the conductivity of the surface layer and T_1 denotes the temperature at the

present time for the first node point below the surface. Letting $D = S + I\downarrow_t - H - E$, the heat balance equation becomes

$$-\varepsilon\sigma T_g^4 + k\left(\frac{T_1 - T_g}{\Delta z}\right) + D = 0$$

or upon rewriting,

$$T_g^4 - \frac{kT_1}{\varepsilon\sigma\Delta z} + \frac{kT_g}{\varepsilon\sigma\Delta z} - \frac{D}{\varepsilon\sigma} = 0$$

The function F is defined by

$$F(T_g) = T_g^4 + \frac{k}{\varepsilon\sigma\Delta z} T_g - \left(\frac{kT_1 + D\Delta z}{\varepsilon\sigma\Delta z}\right) \tag{4}$$

It is seen that the updated surface temperature is a root of F. The Newton-Raphson algorithm has been employed to locate a value of T_g such that F vanishes. In employing the Newton-Raphson scheme, the derivative of F with respect to T_g is needed:

$$\frac{dF(T_g)}{dT_g} = 4T_g^3 + \frac{k}{\varepsilon\sigma\Delta z} - \frac{dD/dT_g}{\varepsilon\sigma} \tag{5}$$

Numerical considerations have resulted in the approximation of dD/dT_g by the following expression

$$\frac{dD}{dT_g} = \frac{(D_N - D_0)}{-\Delta T} \tag{6}$$

where D_N is the value of D using the latest estimate of T_g, D_0 is the value of D obtained by using the previous estimate of T_g, and ΔT denotes the change in temperature. The starting value for the Newton-Raphson scheme is taken to be the surface temperature at the previous time step. It appears that three to five iterations yield satisfactory convergence to the new surface temperature.

Bottom boundary

36. As mentioned in paragraph 27, the bottom boundary condition is the heat flux through the bottom of the lowest layer and can be

specified with one of three options. The requirement of a constant temperature results in a straightforward boundary condition.

37. For options 2 and 3 (see paragraph 27), it is required that the following equation be satisfied:

$$R\downarrow - G - R\uparrow - D = 0 \tag{7}$$

where $R\downarrow$ denotes the radiative energy loss through the bottom boundary, G denotes the heat flux into the lower surface and is given by $G = k(\partial T/\partial x)$ where k denotes the conductivity of the bottom layer, $R\uparrow$ denotes the radiative energy from the constant temperature radiating surface below the bottom boundary, and D is the constant heat flux at the bottom boundary. G is approximated by $k(T_B - T_1)/\Delta z$ where T_B is the temperature of the bottom surface and T_1 is the temperature at the first node point above the bottom surface.

38. The following equation results from substituting the appropriate energy components into Equation 7:

$$\epsilon_B \sigma b_{kB} T_B^4 - k\left(\frac{T_B - T_1}{\Delta z}\right) - \epsilon_R \sigma b_{kR} T_R^4 - D = 0 \tag{8}$$

where ϵ_B denotes the bottom boundary thermal IR emissivity, b_{kB} denotes the bottom geometric shape factor, ϵ_R is the under surface thermal IR emissivity, b_{kR} is the under surface geometric shape factor, and T_R denotes the under surface temperature. Equation 8 is solved by employing the Newton-Raphson iterative scheme.

PART III: COMPUTER PROGRAM INPUT DESCRIPTION AND OPERATION

39. The discussion presented in this Part is intended to serve as both a description of the input files, options, and operation of the TSTM computer code as well as a guide for users of the model. Since all terrain surface feature (material system) and atmospheric condition descriptors and control parameters are a part of the input data file, the discussion is organized around the major types of inputs to the model. Within the discussion of each major input type, the input file format, parameters, parameter units, and relevant control options are presented. Guidance is blended into this framework for data input selection and consideration of the available control options.

40. The input data are read by the program as a single data file consisting of a series of lines of data. Each line of data starts with a line number. Following the line number are the necessary data, coded in a free-field format. The program prints each line of the input data file, excluding the sequential but otherwise arbitrary line number, together with variable name, units, and data category (1 through 8). An example is presented in Figure 2a, and the resulting output is given in Figure 2b. The actual program coding is not presented in this report. However, Appendix A contains a program flowchart and variable definition list for use by readers who have obtained the program code. Typical values for many of the input constants are given in Appendix B. Government agencies can acquire a copy of the code by sending a request to the Commander and Director, WES.

Atmospheric Condition Inputs and Control Options

Atmospheric constants

41. In addition to the line number, the first line of input data contains, in order, atmospheric pressure (millibars), wind speed (metres per second), cloud type index (an integer between 1 and 8), and meteorological instrument shelter height above the surface (centimetres). The shelter height is the height above the surface at which air temperature

and wind speed are measured. Every effort must be made to ensure that the air temperature and wind speed data reflect the conditions at the shelter height above the surface (100-200 cm). Means of adjusting observations to shelter height are available; see, for example, Sellers (1965) or Hess (1959). Because of the empirically determined coefficients in the relations of the model, values for shelter height should fall between 100 and 200 cm. Descriptions of cloud genera and their corresponding cloud type index values are given in Table 1.

Atmospheric hourly data

42. This input information requires 24 lines of data. Each line, in addition to the line number, contains, in order, the 24-hr clock time of the observation, the air temperature (degrees Celsius), relative humidity (percent), cloud cover (tenths, 0.0-1.0), wind speed (metres per second), and total insolation (calories per centimetre squared per minute). Recall that insolation is an optional input; specifically, the model checks the input data to determine if there is a nonzero value for insolation at 1200 hr. If a zero value is encountered, the program then calculates values for insolation using mathematical relationships mentioned in Part II of this report. It is clear that total insolation as an accurate measured input is the more desirable option to be used in the model; however, effects of slope changes on effective insolation must be calculated external to the model if measured values of insolation are input into the program.

Surface-Sun Orientation Specifications

43. In calculating the seasonal and latitudinal insolation changes as well as attenuation due to atmospheric gases and water vapor, the sun's position relative to the surface and zenith angle is needed. As discussed in paragraphs 21 and 22, the orientation of the sun is also employed in calculating the changes resulting from cloud cover and surface slope.

44. For this line of data, there is a line number followed by the

angle (degrees)* of surface slope, surface azimuth angle (degrees), Julian calendar date (integer from 1 to 365), and latitude (degrees).

45. The angle of surface slope is merely the angle between the plane of the surface and the horizontal. The azimuth is the direction of the vector from a unit zenith vector to a unit normal vector. This model uses the convention that south is 0°, increasing positively toward the west and negatively toward the east (Sellers 1965). The Julian calendar date is simply the number of days that have lapsed since 31 December of the previous year.

Heat Flow Calculation Controls

46. This line of input data contains a line number, followed in order by: (a) the number of layers (an integer from one to six); (b) the number of 24-hr repetitions to be run (an integer greater than or equal to one); (c) the time increment (minutes); and (d) the print frequency (minutes).

47. The number of 24-hr repetitions gives the model the number of daily cycles that the user thinks is necessary to "stabilize" the initial temperature profile. If the initial temperature profile is considered accurate, a value of 2 would appear reasonable; whereas, an isothermal input profile may require four cycles. No more than five cycles will ever be required for any realistic case. Each 24-hr cycle is run with the same meteorological conditions and parameters. These repetitions are not to be viewed as a means of enhancing the numerical calculations; i.e., there is no reason to think that by increasing the number of 24-hr cycles, the final results will be improved. In fact, after a "stable" profile has been obtained, further repetitions could, because of computational errors, prove detrimental.

48. The time increment and print frequencies are entered as integral values in minutes. In selecting a time increment, the

---

* A table of factors for converting U. S. customary units of measurement to metric (SI) units is presented on page 3.

stability criterion that $\alpha \Delta t/\Delta z^2 < 1/2$ must be taken into consideration. A time step value of 10 min is considered to be a useful choice for most materials. Thick layers of good insulating materials like dry sandy soil may be well represented at 20- or 30-min steps, but thin layers of high thermal conductivity may require time steps of 5 min or less. It is clear that the print frequency must be greater than or equal to the time increment value.

Material System Descriptors

Initial temperature profile

49. This set of data lines is composed of $k + 1$ lines where k denotes that number of profile points. Specifically, the first line contains in addition to the line number, the number of profile points to be input. The next k lines of data contain the depth (centimetres) below the surface and the temperature of the material at that depth. The only constraint of this series of data is that the bottom profile point must fall within the bottom layer. As discussed in paragraph 42, the number of 24-hr repetitions is related to the accuracy of the temperature profile input into the model.

Top surface constants

50. This line of data contains in order, following the ever present line number: (a) the thermal IR emissivity (0.0 to 1.0) of the top surface; (b) visible wavelength absorptivity (0.0 to 1.0); and (c) the moisture content (0.0 to 1.0).

51. Values of moisture content range from 0.0 (dry) to 1.0 (wet, saturated). Because of the complicated nature of evaporation for non-saturated surfaces (Hess 1959), the user should be cautioned in using intermediate values for this variable. In fact, the user might consider using something such as interval analysis in cases where intermediate values are used.

Layer specification

52. This category of data specifies the computation parameters and thermal properties for each layer of the material to be modeled.

One line of data is used for each material layer, and the lines are ordered from the top layer to the bottom. Each line of data has, as usual, a line number, succeeded in order by the following information layer: (a) layer thickness (centimetres); (b) vertical grid increment (centrimetres); (c) thermal diffusivity (centimetres squared per minute); and (d) thermal conductivity (calories per minute per centimetre per degree Kelvin).

53. If a value less than or equal to zero is read in for the vertical grid increment, for some layer the program will use a default value of one-tenth times the thickness of that layer for the vertical grid increment. Otherwise, the grid increment must be evenly divisible into the layer thickness.

Bottom boundary specifications

54. As indicated in paragraph 28 of this report, the user has the choice of one of three options for the bottom boundary conditions. The initial line of this data set contains a value for the Bottom Boundary Index (BBI), which informs the program which of the three options will be used. Specifically, the three options are selected and defined as follows:

a. Option 1. BBI < 0 ; e.g., -1 indicates that a constant heat flux through the bottom layer is assumed. If this mode is chosen, then the second line of data in this set contains the specified heat flux value (calories per centimetre squared per minute).

b. Option 2. BBI = 0 ; e.g., 0 indicates a constant temperature at the bottom boundary; thus, in this case, the second line of data in this set would be the constant temperature value in degrees Celsius.

c. Option 3. BBI > 0 ; e.g., 1 indicates the option of a constant heat flux at the bottom boundary and an additional constant temperature radiating surface below the bottom boundary.

55. Option 3 is selected if, for example, there is air space below the bottom boundary. For use of option 3, the second data line requires values for six parameters: (a) the constant heat flux value (calories per centimetre squared per minute); (b) the bottom boundary emissivity (0.0 to 1.0); (c) the bottom boundary geometric shape factor

(usually chosen to be 1); (d) the lower radiating surface emissivity (0.0 to 1.0); (e) the lower radiating surface geometric shape factor; and (f) the lower surface temperature in degrees Celsius. Emissivities are the familiar grey body constants that range from 0.0 to 1.0. Geometric shape factors are intended to account for changes of thermal IR emittance and absorption efficiency due to shape. Large flat horizontal surfaces have high values. Small area sources or sinks have small values. A floor in a large room would have a value near 1.0, but a hot motor in that room would have a smaller value. Unfortunately, there is little guidance for an a priori specification of values for the geometric shape factors, other than the value 1.0.

PART IV: SENSITIVITY ANALYSIS AND MODEL VERIFICATION

Sensitivity Analysis

Introduction

56. In almost any application of the TSTM, uncertainties in one or more of the input parameters will exist. This could arise from problems with instruments, uncertainty of the materials in the structure or terrain, or a number of other possibilities. Several of the parameters are difficult to obtain accurately, such as surface saturation. Others, such as cloud cover, require decisions by the user which can be somewhat subjective in nature. All this will usually result in the user dealing with a range of possible temperature predictions rather than a simple number.

57. The range of uncertainty in model output can be established by performing a sensitivity analysis on the variables in question. The sensitivity analysis discussed here provides a starting point for the user to detect suspect parameters by pinpointing variables to which the model is more or less sensitive, and by indicating how the prediction might change for variations in input data. This analysis was performed using a standard set of input data, while varying a test parameter over a range of values characteristic of the specific variable. Plots were then made of the maximum and minimum predicted temperatures versus the value of the test parameter. These plots are contained in Figures 3 to 31. Those curves with large slopes indicate greater model sensitivity to the corresponding parameter, while flatter curves indicate little sensitivity. A summary of the "standard day" used here is given in Figure 32. Also listed are the material parameters for the three-layer system modeled in this analysis.

58. It is emphasized that this sensitivity analysis was performed for only one set of materials under rather artificial conditions. Also, since the analysis of all possible combinations of parameters would be too enormous to be practicable, this study considered univariate changes only. Therefore, the results of the sensitivity analysis should be used

as simply a guide for the analysis of model response to uncertainties in the input data for each case of interest.

Atmospheric parameters

59. The atmospheric parameters used by the model can be divided into two categories: (a) constant and (b) time dependent. The constants are the atmospheric pressure, cloud type, and shelter height. These constants are assumed to remain unchanged over the entire 24-hr period for which the model is run. The data most closely corresponding to the time of interest should be used. The model exhibited very little sensitivity to pressure and shelter height for all values of saturation. The sensitivity analysis of cloud type defined three groups (see Figure 11), types 1 and 2; types 3, 4, and 5; and types 6, 7, and 8. Within each group the model is relatively insensitive, but from group to group the changes can be significant. Of course, cloud type has no effect in the case of zero cloud cover.

60. The time-dependent atmospheric parameters are the air temperature, relative humidity, cloud cover, and wind speed. The sensitivity of these variables was investigated in two parts. The first used constants for all hourly values in each run of the model. Secondly, diurnal variations were introduced into the input time series.

61. The model was found to be highly sensitive to air temperature, with changes in the maximum and minimum predictions that were of the same order as changes in the air temperature. The diurnal variation of the air temperature produced a cycle of temperature estimates only slightly damped compared to the amplitude of the air temperature cycle. The model's sensitivity to relative humidity occurred primarily in the minimum predicted surface temperatures. The maximum values change only 1.5°C over the entire range of relative humidity, while the minimum values vary 5°C (see Figure 8). Increasing saturation increases maximum temperature sensitivity to relative humidity variations.

62. For cloud cover, predictions were made for all cloud types varying cover from 0 to 100 percent for each type except 8. Type 8, fog, has only 0 or 100 percent coverage. The model's sensitivity to cloud cover was found to increase with an increase in cloud cover and

in the index values of the cloud type, as expected. The model is relatively insensitive to any cover for type 1, but temperatures vary more than 10°C over the 0 to 100 percent range for type 7. The model predictions throughout the day are sensitive to cloud cover variations, as seen in Figures 25 and 26.

63. The sensitivity of the model to wind speed is primarily in the maximum predicted temperatures, with the minimum changing less than 1°C over a wide range of wind speeds. However, as indicated in Figure 27 and 28, the model does respond to change of wind speed with time. This is also true for cases of nonzero saturation, although the magnitude of the predicted temperatures decreases. The diurnal variation of the predictions indicates that the model is, in this case, insensitive to wind speed variations at night when sensible and latent heat transfers are minimal or zero.

Site characteristic parameters

64. The site characteristic parameters consist of all information supplied to the program describing the specific structure or terrain to be modeled. This includes data on the geographic location, surface orientation, time of year, initial conditions, bottom boundary conditions, and material properties. The model was not tested for sensitivity to surface orientation, geographic location, or time of year since these are exact calculations used in estimating insolation. However, users who must estimate insolation in cases where these inputs are not exactly known should consider performing a brief sensitivity analysis on these parameters for their particular case. Under some circumstances surface temperatures are quite sensitive to site characteristics.

65. The initial temperature profile establishes the initial heat conditions throughout the materials. Relatively small changes in this profile (thus, material heat storage) can result in drastic differences in predicted temperatures (Figure 10). Problems with this parameter may be recognized by observing the predicted temperatures at the beginning and end of the modeled day. Both numbers should be the same, if the system has reached equilibrium. If not, the user may increase the number of 24-hr repetitions made before printout (see Part III). The best

solution is, of course, in using a more accurate temperature profile.

66. The model exhibited little sensitivity to the bottom boundary conditions when expressed as a temperature, varying over a 20°C range. However, the effect of this parameter could change significantly when imposed at smaller depths than used in this analysis or for more highly conductive materials. When expressed in terms of a net heat flux, variations in the bottom boundary conditions did cause small changes in the predicted temperature--increases for ingoing flux and decreases for outgoing. Again, this effect will be more pronounced for shallower bottom boundary depths. No sensitivity analysis was performed for the case of an air space below the lower boundary (paragraph 28), but tests were made to ensure the correctness of the calculation.

67. The material parameters consist of data supplied for each layer of the structure of terrain and information needed for the surface only. Thickness, thermal diffusivity, and heat conductivity must be specified for each layer. The model's sensitivity to thickness variations is related to the layer's heat conductivity, with higher values resulting in less change with thickness than lower values. For constant layer thickness and thermal diffusivity, increasing heat conductivity causes a narrowing of the range of predicted temperatures. Variations in thermal diffusivity (Figure 20) produce very little change in model predictions. This parameter is directly involved only in the calculation of the numerical stability factor described in Part II. Values for heat conductivity and thermal diffusivity for several materials and ground cover are listed in Appendix B.

68. The surface parameters are the thermal infrared emissivity, solar absorptivity, and fractional saturation of the surface material. The model exhibits a significant sensitivity to emissivity in both the minimum and maximum predicted temperatures, with both decreasing for higher emissivities. Variations in solar absorptivity cause large changes in the predicted maximum temperatures, which increase almost 20°C over the 0 to 1 range of absorptivity. The minimum temperature remained relatively constant, however, increasing 3°C over the entire range of absorptivity (see Figure 23). For saturated materials, the

minimum predicted temperatures change very little, but maximum values decrease by more than 8°C over the 0 to 1 range of saturation. Although not investigated in this analysis, it should be recognized that changes in saturation may cause variations in the true top layer heat conductivity, thermal diffusivity, emissivity, and absorptivity. No provision for automatically modifying these parameters for effects of saturation is included in the program, so the user must change the input data to account for these effects.

Numerical procedures
control parameters

69. The numerical control parameters are the time step, the grid spacing (which must be specified independently for each layer), and the number of 24-hr repetitions to be performed before printout. The time step and grid spacing are used in the calculation of the numerical stability parameter Λ, as shown below:

$$\Lambda = \alpha_i \frac{\Delta t}{\Delta z_i^2}$$

where

α_i = thermal diffusivity for i^{th} layer

Δt = time step

Δz_i = grid spacing for i^{th} layer

In order for numerical stability to be assured, Δt and Δz must be selected so that Λ is less than or equal to 1/2. For a large diffusivity, the ratio of Δt to Δz^2 must be small. This can result in very small time steps in the case of a highly conductive thin layer because Δz must be very small. Analysis of top layer thickness indicates that thin, highly conductive layers may usually be neglected for multilayer systems. For example, in the case of a 2-mm-thick metal plate, a temperature gradient of only 0.5°C is created across the layer (Bornemeier, Bennett, and Horvath 1969). Variation of Δt and Δz for constant diffusivity and stability factor $\leq 1/2$ shows that the model has essentially no sensitivity to these parameters provided that no numerical instability is encountered because Δt or Δz is too large.

Figure 24 shows Δt versus Δz for several values of thermal diffusivity.

70. The number of 24-hr repetitions needed is directly related to the accuracy of the initial temperature profile. The analysis of the model's sensitivity to this parameter indicates that when the initial temperature profile is close to the equilibrium conditions, predictions are insensitive to repetitions beyond a period of 2 to 4 days. Uncertainty in the initial profile can be countered to some extent by increasing the number of 24-hr repetitions.

71. In Table 2 the input parameters are categorized according to the degree of sensitivity displayed by the model. The model exhibits little sensitivity to some parameters, so it appears that relatively rough approximations can be used for these with confidence. Above all, any user should recognize that this model is not expected to produce temperature predictions with absolute accuracy, irrespective of the correctness of the input data. There are simply too many complex processes in nature for any model of practical usefulness to take into account. The greatest value is in predicting trends for such uses as estimating contrast between two dissimilar objects or relative changes over time. Take, for example, the case of contrast prediction between a structure and the surrounding terrain. Errors from poor specification of atmospheric parameters will be common to both features. Here, the most important parameters would be those which are different for the structure and terrain, such as heat conductivity and saturation. The user must keep considerations such as these in mind when evaluating the uncertainties of model estimates for a specific purpose.

Model Verification

Technique

72. A mathematical model is only useful if it is an accurate abstraction of the phenomena modeled. An important aspect of the development of a model, therefore, is to verify that the model provides realistic answers for the conditions or bounds within which it is to be applied.

One method of model verification is to compare values predicted by the model to measured values, the inputs to the model representing the conditions under which the measured values were obtained. This is a rather simplistic verification because only the final model output is used as a yardstick to judge the ability of the model to realistically represent the phenomena abstracted in the model. This method also dictates that values for the model inputs and outputs are measured very carefully and in most instances simultaneously. As already pointed out, acquiring such input and reference output values is often a very difficult task and characteristically such data are seldom readily available unless a specific effort has been made to obtain them. In many instances it is difficult to accurately measure all of the necessary values because of a lack of equipment or other resources.

73. In spite of the shortcomings mentioned in the previous paragraphs, the method described was used to conduct a limited verification of the TSTM. Since many model users only concern themselves with model outputs, usually as input to the solution of some broader or more sophisticated problem, it does provide direct and visible evidence of model applicability and accuracy.

Test data

74. Two terrain surfaces were used for the verification test--a concrete pad and a bare soil patch within a grass-covered area, both located near the Environmental Laboratory Headquarters building at WES. Weather data consisting of wind speed, wind direction, total insolation, air temperature, relative humidity, and precipitation were measured at 10-min intervals for the period 28 July 80 to 5 August 80. Surface temperature measurements for the concrete pad and bare soil surfaces were also made at 10-min intervals coincident with the weather data. The surface soil temperature was measured with a thermistor buried approximately 1 cm below the soil surface, and the concrete surface temperature was measured with a thermistor attached to the surface of the concrete pad.

75. All weather and temperature data described in the above paragraph were recorded on Campbell Scientific Model CR21 Microloggers.

All weather measurements were made at a height of 2 m above the ground. Physical entities such as concrete pad thickness, soil type, soil layering, initial soil temperature profiles (with depth) and visual reflectance coefficients of the concrete and soil surfaces were measured. Values for heat conductivity, thermal diffusivity, and absorptivity were estimated from the literature (Link 1979). Cloud cover and cloud type observations were made periodically during daylight hours only and assumed to be constant for both days.

76. Weather data for 31 July 80 and 5 August 80 were selected for the verification test. Two days were selected to provide some measure of repeatability. Table 3 is a listing of the weather data. Table 4 is a listing of the material property values used for the concrete pad and bare soil. The concrete pad was modeled as a 10-cm layer of portland cement concrete over a 15-cm layer of sandy soil. The bare soil patch was modeled as a single 50-cm layer of uniform silt.

Model predictions

77. The TSTM was used to predict surface temperature values for the bare soil and concrete pad using the weather data for 5 August 80 (Table 3) and for the bare soil using the weather data for 31 July 80. The model-predicted temperature values were then plotted against measured values for a 24-hr cycle. Figures 33, 34, and 35 present the predicted and measured temperature plots for the concrete pad, bare soil on 5 August 80, and bare soil on 31 July 80, respectively. Air temperature is included on the bare soil temperature plots (Figures 34 and 35).

Discussion

78. The TSTM-predicted temperatures for the concrete pad (Figure 33) were virtually always within 2°C of the measured values. Perhaps even more significant was the close match of the predicted and measured values for the peak and rising and falling portions of the diurnal cycle. Throughout the nighttime hours the predicted values were consistently 2°C cooler than the measured values. This may be due to such things as cloud cover conditions that were not observed during nighttime hours, or an insufficient representation of sensible

heat exchange during nighttime hours. Otherwise, the observed temperature differentials are on the order of the uncertainty of the measured data.

79. The predicted and measured values for the bare soil patch (Figures 34 and 35) did not match as closely as those for the concrete pad. The model estimates were consistently cooler than the measured values during the nighttime hours by 2 to 3°C. Daytime values were more closely matched, especially for the 31 July 80 diurnal cycle. In both Figures 34 and 35 the measured values lag the predicted values; this is especially evident on the rising portion of the diurnal cycle. It is hypothesized that this lag resulted because the soil temperature measurements were made at about 1 cm below the true surface (paragraph 74). There is characteristically a strong temperature gradient with depth below the surface, and the temperature fluctuations below the surface lag those at the surface. Thus, the actual surface temperatures and the model predictions of those temperatures would tend to respond more rapidly to changes in the weather over the diurnal cycle. The peak temperature values were within approximately 1 to 2°C on both days, which is on the order of uncertainty for the measured values.

80. A very important criteria for the TSTM is the capability to predict reasonable temperature contrast values for different terrain surface scene elements. To examine the ability of the TSTM to generate contrast values, the data for Figures 33 and 34 were combined and plots of the temperature difference (contrast) between the concrete pad and bare soil were generated for both the predicted and measured values. Figure 36 shows a comparison of the predicted and measured contrast values. The curves in Figure 36 very closely match, indicating that the TSTM did a good job of predicting contrast. The match is especially close during the 0 to 1600 hr period. The relatively larger differences for the period of 1600 to 2400 hr can be explained to some extent by the lag of soil temperature measurements as discussed in paragraph 79. It is important that the model was able to represent rapid transient changes of contrast.

PART V: CONCLUSIONS AND RECOMMENDATIONS

Conclusions

81. The material designer or evaluator generally chooses to work with the simplest definition of an operational environment that seems practical. In the case of surveillance, target acquisition devices, or camouflage measures, a single number for target-to-background contrast is often the criteria used for design or evaluation. Because the target and the background are often both dynamic, the contrast value is also dynamic. The balance between simplicity and reality must be carefully considered and every effort made to generate the capability to provide the material development community with realistic design criteria in a cost-effective manner. The AWGTSP is focused on this broad objective, and the mathematical modeling efforts ongoing such as that reported herein are the foundation for providing the tools necessary to reach this objective. Realism must be paramount and should remain the major focus of data base development and modeling efforts.

82. The TSTM is a step forward in the effort to realistically project the thermal signatures of terrain surface (nonvegetative) features that are commonly background for targets or items to be camouflaged. The model can be applied with either actual or hypothetical data and has been shown to produce realistic outputs over a range of atmospheric and material system conditions. Although the TSTM is a one-dimensional model, it can be used to examine background features in a variety of situations. Difficulties arise in attempting to model vertical walls and steeply sloped surfaces. Other modeling alternatives are being examined for these situations. Most natural nonvegetative features are readily abstracted to layered systems with horizontal or moderately sloping surfaces.

83. The major advancements offered by the TSTM are realistic consideration of cloud cover and cloud type, the capability to simulate the effects of fast and/or transient changes of environmental conditions, simplistic inputs describing the feature and atmospheric conditions, and

applicability over a broad spectrum of weather and seasonal conditions and material characteristic values. The major difficulty in applying the model is the acquisition of accurate values for material descriptors such as heat conductivity and thermal diffusivity. Some materials such as portland cement concrete can vary considerably in their thermal properties because of differences in the characteristics of individual components.

Recommendations

84. The version of the TSTM presented in this report represents the completion of a phase of model development. Knowledge gained during this phase combined with an increasing awareness of its short- and long-term application suggest several directions for continued modeling advancement. The completion of a model development phase also calls for complementary experimental work to evaluate the present model and to guide future effort.

85. The model contains a number of assumptions and simplifications which potentially limit the model's validity. These limits need to be determined, and conditions where the model is not valid must be defined. Theoretical considerations are helpful, but, in the end, the model must be tested against carefully obtained experimental data. It is recommended that data sets be obtained and analytical effort be supplied to provide reasonable demonstration and definition of model validity. (This is no trivial task; a complete experimental validation requires data covering all combinations of all controlling variables over their full range of values. Accurate measurements are not easily made. Realistic time and effort constraints preclude a total model validation/verification effort.)

86. Layered systems are common on the earth's surface, making the TSTM a widely applicable tool. In many instances, however, the terrain surface is partially or wholly covered with a grass canopy. While vegetation canopy models are available, they require careful specification of intracanopy meteorological conditions, canopy structure, and

biophysical characteristics. The general canopy signature problem is complex, but it is likely that a simple module can be developed for the TSTM that can handle simple herbaceous canopies under moderate environmental conditions. The TSTM could then be applied to areas such as rangelands, pastures and lawns. It is recommended that a simplistic herbaceous canopy module for the TSTM be developed and tested.

87. Prediction of surface temperatures is only the first step in the prediction of thermal IR signatures. Surface temperatures and spectral emissivities are required to determine spectral radiance. The effects of the atmosphere on this radiation must then be considered, followed by the application of a sensor response model. Knowledge of spectral emissivity of terrain materials is incomplete and unorganized. It is important that available data be collected and that the remaining gaps be filled. Atmospheric transmission modeling work is currently ongoing through the U. S. Army Atmospheric Sciences Laboratory. Their efforts are particularly important in that they are creating an engineering-type model that handles the complex multiple scattering phenomenon that is significant in dusty and smoky battlefield environments. This model should be built into the signature prediction process.

88. Consideration should be given to the development of an implicit scheme for the solution of the heat transfer equation. Such a scheme would be unconditionally stable, thereby expanding model applicability and simplifying model operation.

89. The TSTM is currently one-dimensional. While this configuration can handle many situations (many features) that occur in nature, there is a class of features that may require a two- or three-dimensional modeling capability. These are features that can be mistaken for targets, creating false alarms or false target acquisition. Examples might include large rocks, cultural features with dimensions of the same order of magnitude as a target, or small individual facilities that are to be camouflaged. It is recommended that research be conducted to investigate the specific need for a multidimensional modeling capability for false target features. The work should be focused on the magnitude of errors that occur from applying one-dimensional models for these features, the

potential improvement offered by multidimensional models development of prototype multidimensional models, and more verification for specific features.

REFERENCES

American Society of Heating, Refrigerating, and Air-Conditioning Engineers. 1977. 1977 Fundamentals, ASHRA Handbook, New York.

Bornemeier, D., Bennett, R., and Horvath, R. 1969. "Target Temperature Modeling," University of Michigan, under contract to the U. S. Air Force, contractor report No. 1588-5-F.

Buettner, K J. K. and Kern, C. D. 1965. "The Determination of Infrared Emissivities of Terrestrial Surfaces," Journal of Geophysical Research, Vol 70, No. 6, pp 1329-1337.

Carnahan, B. H., Luther, A., and Wilkes, J. O. 1964. Applied Numerical Methods, Vol 2, John Wiley and Sons, Inc., New York, pp 431-781.

Haurwitz, B. 1948. "Insolation in Relation to Cloud Types," Journal of Meteorology, Vol 5, pp 1673-1680.

Hess, S. L. 1959. Introduction to Theoretical Meteorology, Holt, Rinehart, and Winston, New York.

Jumikis, A. R. 1977. Thermal Geotechnics, Rutgers University Press, New Brunswick, N. J.

Khale, A. B. 1977. "A Simple Model of the Earth's Surface for Geologic Mapping by Remote Sensing," Journal of Geophysical Research, Vol 82, No. 11, pp 1673-1680.

Lamb, R. C. 1974. "The Radiation and Energy Balance on a Burned vs. an Unburned Natural Surface," presented to the Conference on Fire and Forest Meteorology of the American Meteorological Society and the Society of American Foresters, April 2-4, 1974.

Link, L. E. 1979. "Thermal Modeling of Battlefield Scene Components," Miscellaneous Paper EL-79-5, U. S. Army Engineer Waterways Experiment Station, CE, Vicksburg, Miss.

Murry, F. W. 1967. "On the Computation of Saturation Vapor Pressure," Journal of Applied Meteorology, Vol 6, pp 203-204.

Oke, T. R. 1978. Boundary Layer Climates, Methven and Co. Ltd., Halsted Press Book, John Wiley and Sons, New York, pp 322-334.

Pochop, L. O., Shanklin, M. D., and Horner, D. A. 1968. "Sky Cover Influence on Total Hemispheric Radiation During Daylight Hours," Journal of Applied Meteorology, Vol 7, pp 484-489.

Sellers, W. D. 1965. Physical Climatology, University of Chicago, Ill.

Small, J. T. 1977. "A Theoretical Analysis of Changes in Thermal Signatures Caused by Physical and Climatological Factors." Master's Thesis, Air Force Institute of Technology, Colorado Springs, Colo.

Smith, J. A., Ranson, K. J., Nguyen, D., and Link, L. E. 1980. "Thermal Vegetation Canopy Model Studies, Final Report," Colorado State University, Fort Collins, Colo.

Smith, W. L. 1966. "Note on the Relationship Between Total Precipitable Water and Surface Dew Point," Journal of Applied Meteorology, Vol 5, pp 726-727.

Wechsler, A. E. and Glaser, P. E. 1966. "Surface Characteristics Effect on Thermal Regime, Phase I," Special Report 88, U. S. Army Materiel Command, Cold Regions Research and Engineering Laboratory, Hanover, N. H.

Table 1

Cloud Genera and Cloud Type Indexes*

Cloud Genera	Abbreviation	Index Value	Comments
Cirrus	Ci	1	High clouds composed of white delicate filaments, patches of narrow bands, elements often curved or slanted and smaller than Cs, never overcast or precipitating
Cirrostratus	Cs	2	High clouds appearing as whitish veil usually fibrous, often produces halo phenomena, thinner than As, does not appear to move, nonprecipitating
Altocumulus	Ac	3	Midlevel clouds, patches, usually broken, lee wave clouds, elements smaller than Sc, nonprecipitating
Altostratus	As	4	Midlevel grey sheet or layer of striated, fibrous or uniform appearance, large horizontal extent; thicker than Cs, thinner than Ns, precipitation generally light and continuous (if any)
Stratocumulus	Sc	5	Grey and/or whitish layer or patch, nearly always has dark spots and is nonfibrous; elements larger than Ac, nonprecipitating
Stratus	St	6	Grey rather uniform base, patches ragged if present, precipitation unusual but light and continuous if present, lower and more uniform than Sc, less dense and less "wet" than Ns
Nimbostratus	Ns	7	Grey often dark, diffuse, large horizontal and vertical extent, thicker than As, more uniform than Sc, often precipitating, precipitation continuous
Fog	Fg	8	

* Cloud genera; Cumulus (Cu), Cirrocumulus (Cc), and Cumulonimbus (Cb) are not treated here. At low cloud covers (≤ 0.3), Cu and Cc may be approximated with Ac.

Table 2

Relative Model Response to Variation of Input Parameters

Very Sensitive	Moderately Sensitive	Very Insensitive
Air temperature	Relative humidity	Air pressure
Solar absorption	Shelter height	Cloud cover (types 1,2)
Thermal emissivity	Wind speed	Thermal diffusivity
Initial temperature profile	Cloud cover (3,4)	Time step*
Saturation	Cloud type: (group to group (1,2) (3,4,5) (6,7,8)	Grid spacing*
Cloud cover (types 5,6,7)		24-hr repetitions
Top layer heat conductivity		Bottom boundary flux**

* Not sensitive, provided model is numerically stable.

** Not sensitive for thick systems with relatively low heat conductivity.

Table 3

Measured Weather Data for Model Verification

Time of day hr	Air Temperature °C 31 Jul/5 Aug	Relative Humidity percent 31 Jul/5 Aug	Cloud Cover (0.0-1.0) 31 Jul/5 Aug	Wind Speed m/sec 31 Jul/5 Aug	Solar Insolation w/m^2 31 Jul/5 Aug
0	23.5/24.8	83.9/90.0	0.3/0.3	0.8/0.5	0/0
1	22.3/24.5	89.5/91.0	0.3/0.3	0.5/0.5	0/0
2	21.7/24.1	90.8/91.0	0.3/0.3	0.5/0.4	0/0
3	21.6/23.9	91.0/90.0	0.3/0.3	0.4/0.5	0/0
4	21.5/23.6	91.4/91.0	0.3/0.3	0.5/0.7	0/0
5	21.6/23.2	91.5/91.0	0.3/0.3	0.6/0.4	0/0
6	21.0/23.2	91.9/91.0	0.3/0.3	0.5/0.4	0/0
7	21.9/23.4	91.8/91.0	0.3/0.3	0.5/0.5	3/39
8	23.8/26.4	89.6/85.0	0.3/0.3	0.8/1.0	22/218
9	28.2/29.0	81.6/80.0	0.3/0.3	1.3/1.9	44/236
10	30.6/31.4	76.6/74.0	0.3/0.3	1.3/1.8	60/607
11	32.0/33.0	68.3/68.0	0.3/0.3	1.9/1.7	802/767
12	33.3/34.5	64.8/66.0	0.3/0.3	1.6/1.7	784/855
13	34.1/35.7	60.0/59.0	0.3/0.3	1.6/1.4	779/905
14	34.8/36.1	57.7/58.0	0.3/0.3	1.6/1.2	874/681
15	36.0/36.9	55.6/52.0	0.3/0.3	1.5/1.6	812/867
16	35.6/37.2	52.1/53.0	0.3/0.3	1.3/1.5	651/741
17	35.9/37.5	55.2/48.0	0.3/0.3	1.0/1.2	342/443
18	34.1/36.5	55.9/52.0	0.3/0.3	1.1/0.9	494/316
19	30.9/34.4	63.7/63.0	0.3/0.3	1.5/0.8	237/114
20	27.3/28.2	76.4/67.0	0.3/0.3	1.2/2.1	12/12
21	25.5/23.4	82.0/90.0	0.3/0.3	1.1/0.9	0/0
22	25.0/23.3	84.0/91.0	0.3/0.3	0.8/0.7	0/0
23	24.2/22.9	85.6/91.0	0.3/0.3	0.6/0.8	0/0
24	23.0/22.5	89.1/91.0	0.3/0.3	0.6/0.7	0/0

Pressure mb 31 Jul/5 Aug	Cloud Type 31 Jul/5 Aug	Shelter Height cm 31 Jul/5 Aug
1000.0/1000.0	3/3	200/200

Table 4

Material Parameter Values for Model Verification

	Concrete Pad		Bare Soil
	Layer 1	Layer 2	
Thickness, cm	10	15	50
Thermal diffusivity, cm^2/min	0.37	0.32	0.29
Thermal conductivity, cal/min-cm-°K	0.13	0.16	0.25
Longwave emissivity	0.90	--	0.92
Shortwave absorptivity	0.80	--	0.75
Surface saturation	0.0	--	0.5
Temperature profile			
Depth, cm; temperature, °C	0.0, 28.1		0.0, 29.4
	23.0, 32.0		15.0, 31.6
	--		23.0, 31.3
Bottom boundary temperature, °C	32.0		30.0

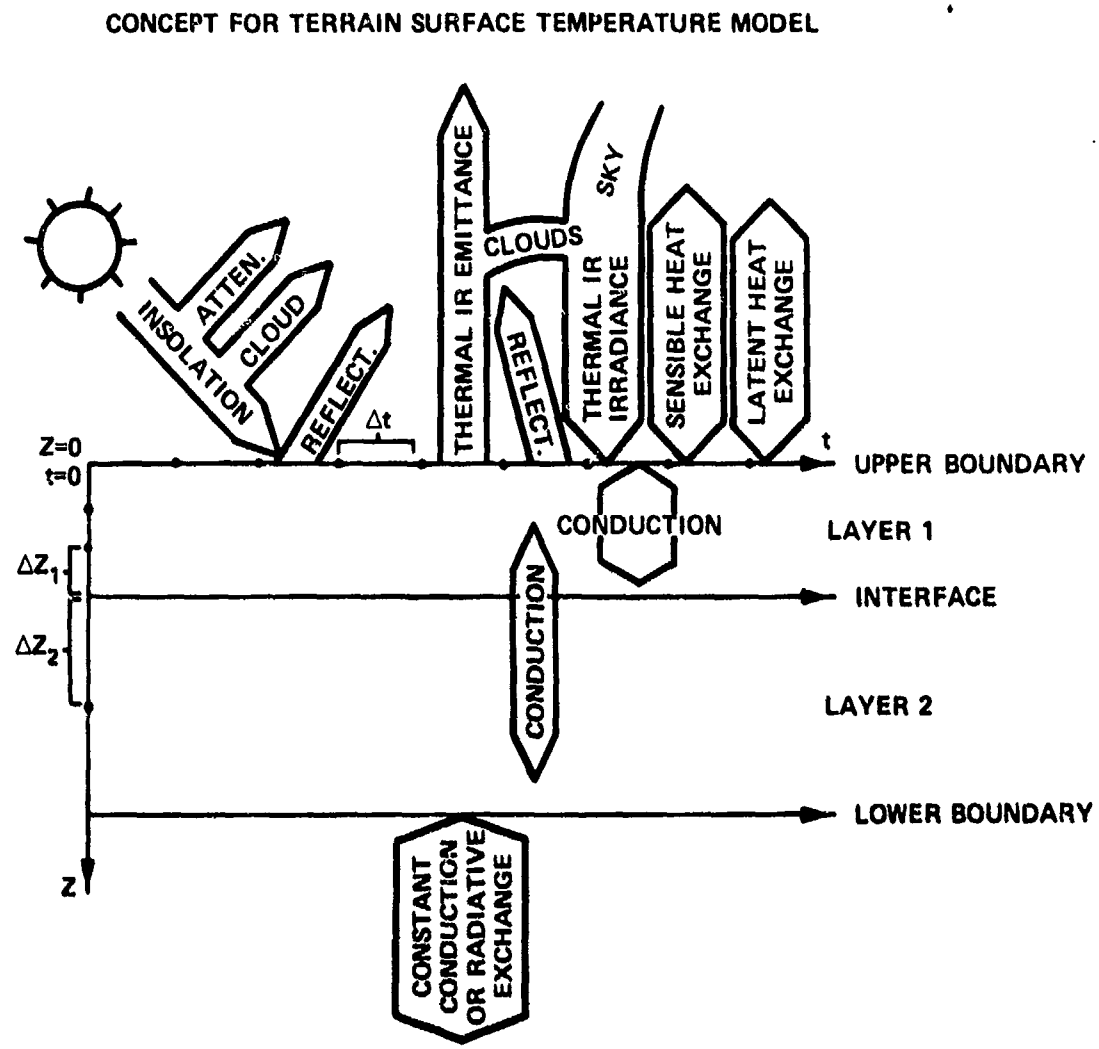

Figure 1. Terrain Surface Temperature Model

ATMOSPHERIC-SPECIFICATIONS

ATMOS PRESS MB	CLOUD TYPE INDEX	SHELTER HEIGHT-CM
972.6	3	175.00

TIME HR	AIR TEMP DEG C	RH %	CLOUD COVER (0-1)	WIND SPEED M/S
1.0	7.1	76.4	0.8	0.6
2.0	6.9	76.4	0.8	0.7
3.0	6.9	76.4	0.8	0.5
4.0	7.0	76.4	0.8	0.4
5.0	7.0	81.8	0.8	0.7
6.0	7.1	81.8	0.9	2.1
7.0	7.1	81.8	0.9	2.6
8.0	8.6	81.8	0.9	2.7
9.0	9.2	81.8	1.0	3.1
10.0	9.8	76.6	0.9	3.1
11.0	10.4	71.7	1.0	3.2
12.0	10.1	71.7	1.0	2.8
13.0	10.2	71.7	0.9	3.1
14.0	10.1	71.7	1.0	3.5
15.0	9.8	76.6	1.0	2.9
16.0	9.8	76.6	1.0	3.4
17.0	9.1	76.6	1.0	3.8
18.0	8.8	81.8	1.0	2.9
19.0	8.5	81.8	1.0	2.6
20.0	8.4	81.8	1.0	2.1
21.0	8.3	81.8	1.0	2.1
22.0	8.0	87.4	1.0	1.3
23.0	7.9	87.4	1.0	2.0
24.0	7.1	76.4	0.8	0.6

SURFACE-ORIENTATION-SPECIFICATIONS

SFC SLOPE DEG-HORIZ = 0	SFC AZIMUTH DEG S=0	DAY JULIAN	LATITUDE DEG
0	0	265.0	49.2

HEAT-FLOW-CALCULATION-CONTROLS

NO. OF LAYERS 1-6	NO. OF 24 HR REPETITIONS	TIME STEP MIN	PRINT FREQ MIN
2	3.0	5.	60.

INITIAL-TEMPERATURE-PROFILE

NUMBER OF PROFILE POINTS = 3

DEPTH CM	TEMP DEG C
0	10.6
20.0	14.0
30.0	14.0

TOP-SURFACE-CONSTANTS

EMISS	ABSORP	SATURATION
0.95	0.85	0.

INPUT-LAYER-SPECIFICATIONS

LAYER NO.	THICKNESS CM	VERT. GRID SPACE CM	THERMAL DIFF CM**2/MIN	HEAT COND CAL/MIN-CM-K
1	20.0	5.0	0.23	0.11
2	10.0	5.0	0.32	0.16

INPUT BOTTOM BOUNDARY DATA

BOTTOM BOUNDARY INDEX = 0
BOTTOM BOUNDARY TEMPERATURE = 14.0 DEG C

a. Example input data for TSTM

Figure 2. Input data and output for TSTM (Continued)

HR	SURFACE TEMP DEG C	GRAYBODY RADIANCE	SOLAR INSOLATION	SURFACE ABSORP (W/M**2)	ATMOS IR EMISSION	SENSIBLE HEAT LOSS	LATENT HEAT LOSS
0.00	7.3	333	0	0	287	1	0
1.00	6.8	330	0	0	286	0	0
2.00	6.3	328	0	0	285	0	0
3.00	6.2	328	0	0	289	0	0
4.00	6.1	327	0	0	290	0	0
5.00	6.0	327	0	0	292	0	0
6.00	6.6	329	0	0	300	2	0
7.00	9.2	342	87	73	300	26	0
8.00	13.3	362	198	168	310	69	0
9.00	15.6	374	252	214	322	107	0
10.00	19.1	392	393	334	314	174	0
11.00	19.7	386	367	311	326	176	0
12.00	20.3	399	383	325	324	192	0
13.00	21.4	405	447	379	314	225	0
14.00	19.3	393	323	274	324	179	0
15.00	17.9	386	252	214	324	142	0
16.00	15.7	374	164	139	324	101	0
17.00	12.6	359	68	57	320	59	0
18.00	10.6	348	0	0	320	22	0
19.00	9.9	345	0	0	318	16	0
20.00	9.6	344	0	0	317	11	0
21.00	9.3	342	0	0	316	9	0
22.00	9.1	341	0	0	316	8	0
23.00	8.8	340	0	0	316	8	0
0.00	7.3	333	0	0	287	1	0

b. Output for TSTM

Figure 2. (Concluded)

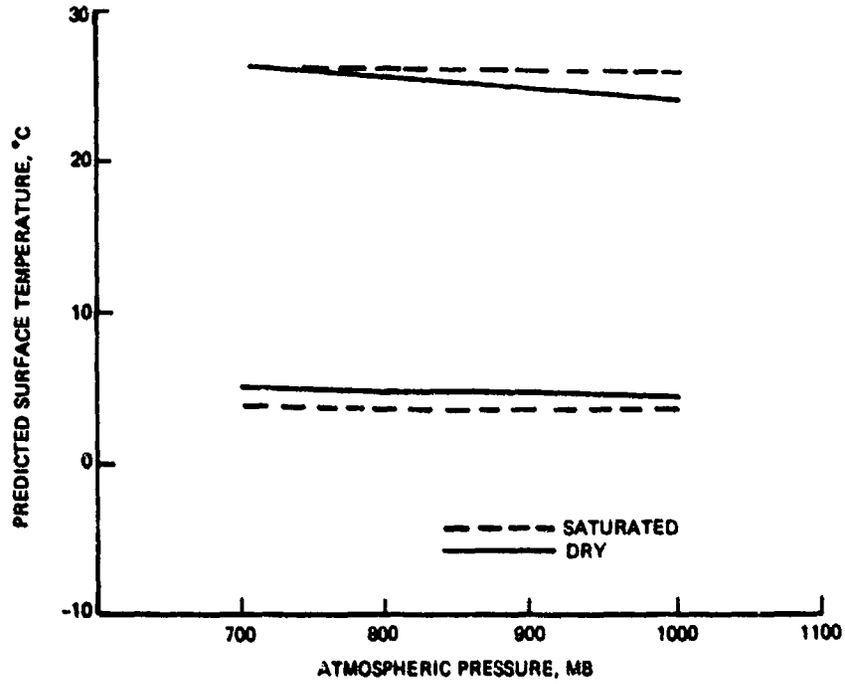

Figure 3. Changes in max-min temperature predictions for variations in atmospheric pressure

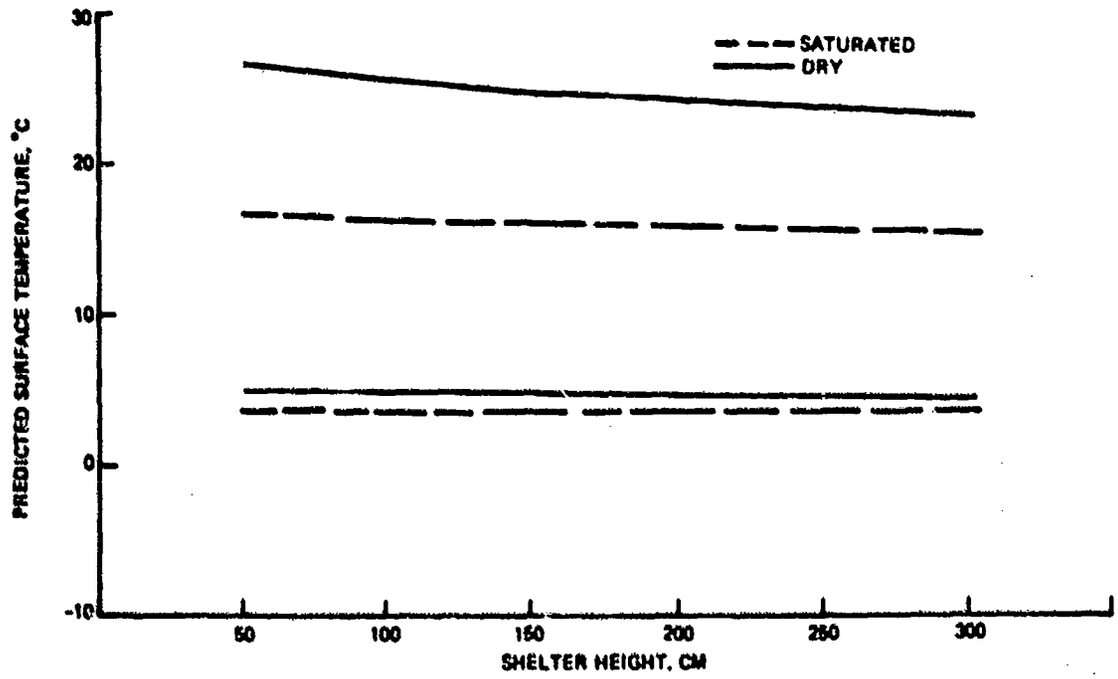

Figure 4. Changes in max-min temperature predictions for variations in instrument shelter height

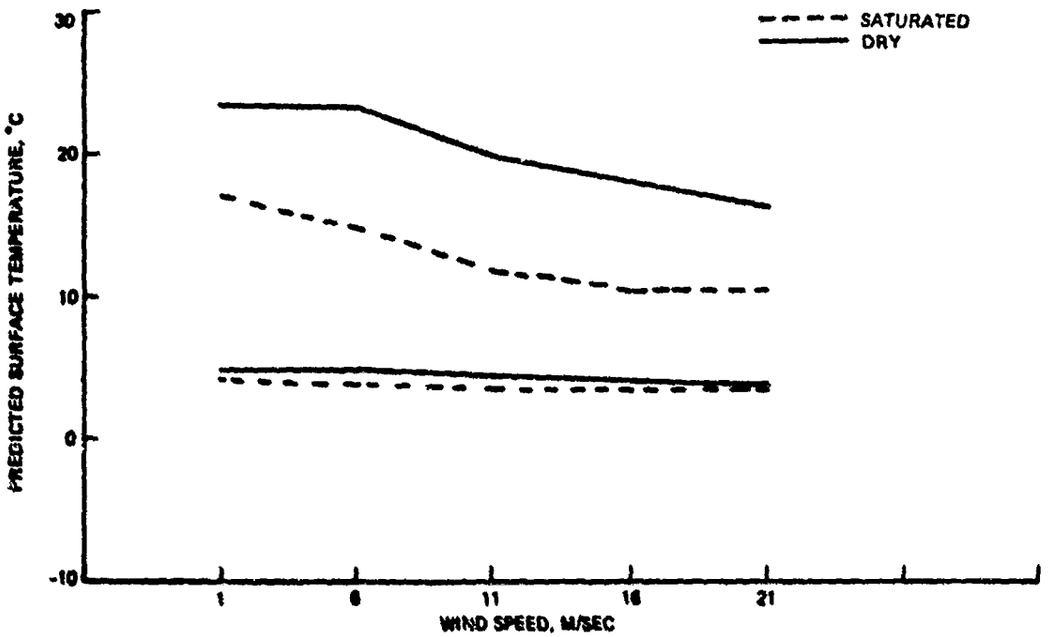

Figure 5. Changes in max-min temperature predictions for variations in wind speed

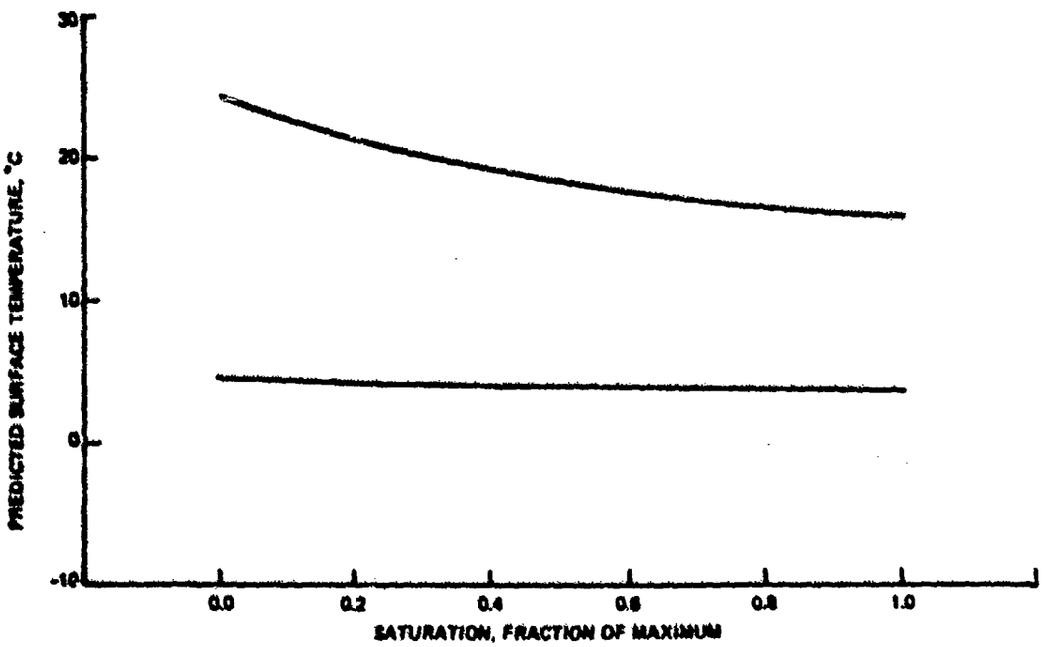

Figure 6. Changes in max-min temperature predictions for variations in surface saturation

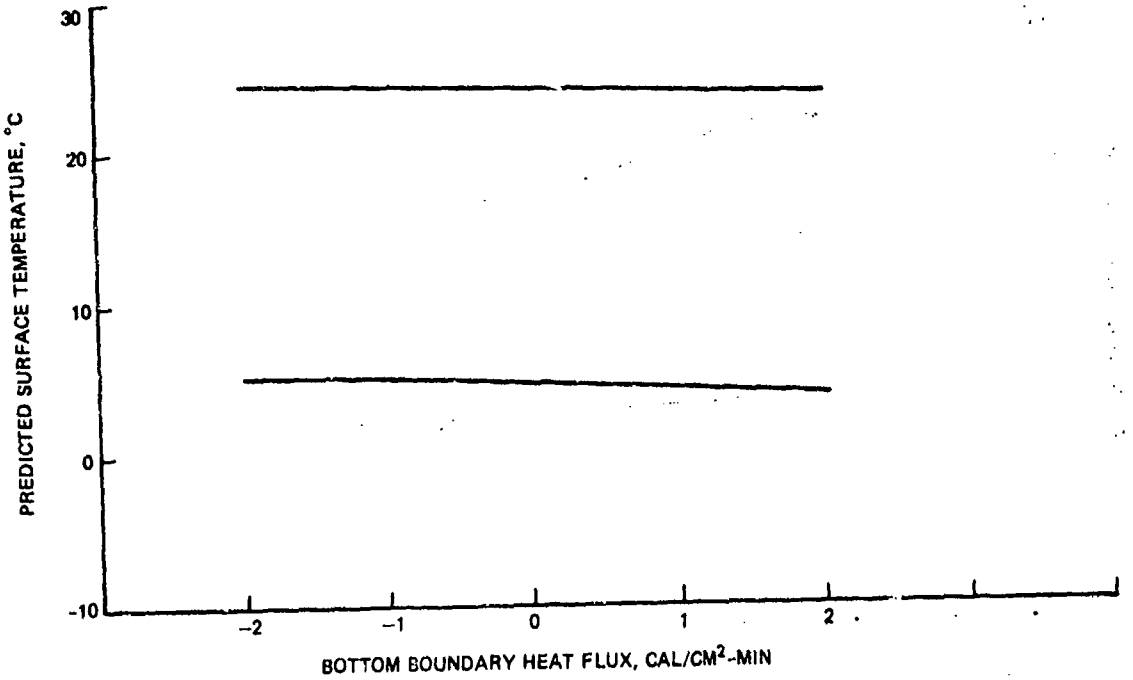

Figure 7. Changes in max-min temperature predictions for variations in the bottom boundary heat flux

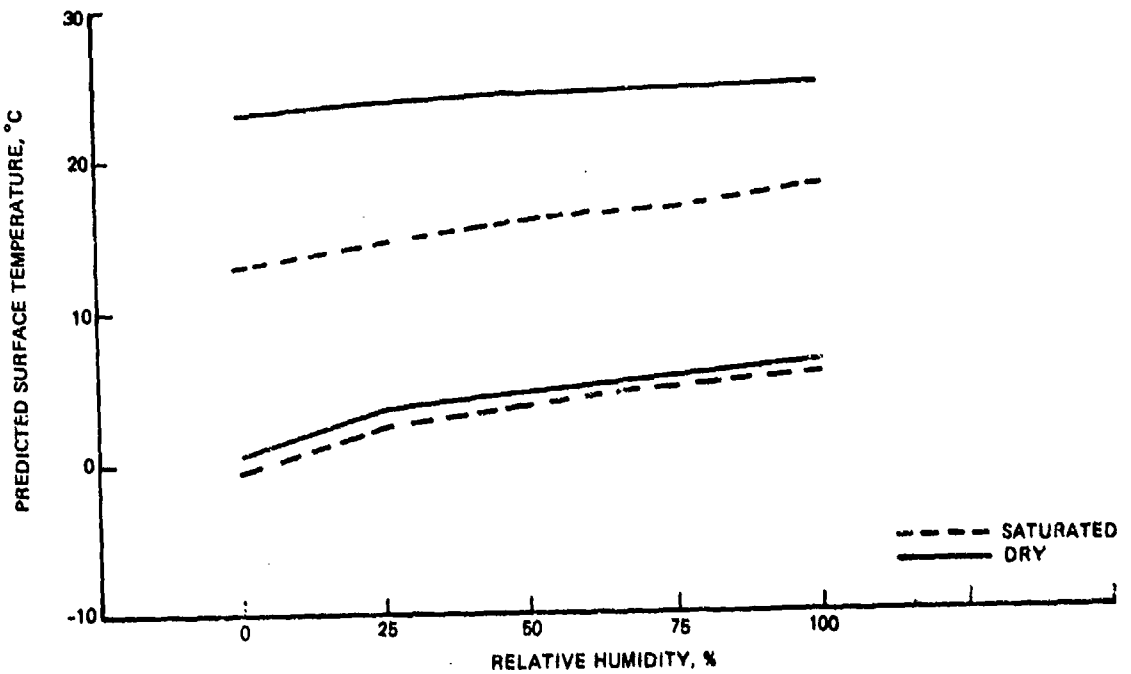

Figure 8. Changes in max-min temperature predictions for variations in relative humidity

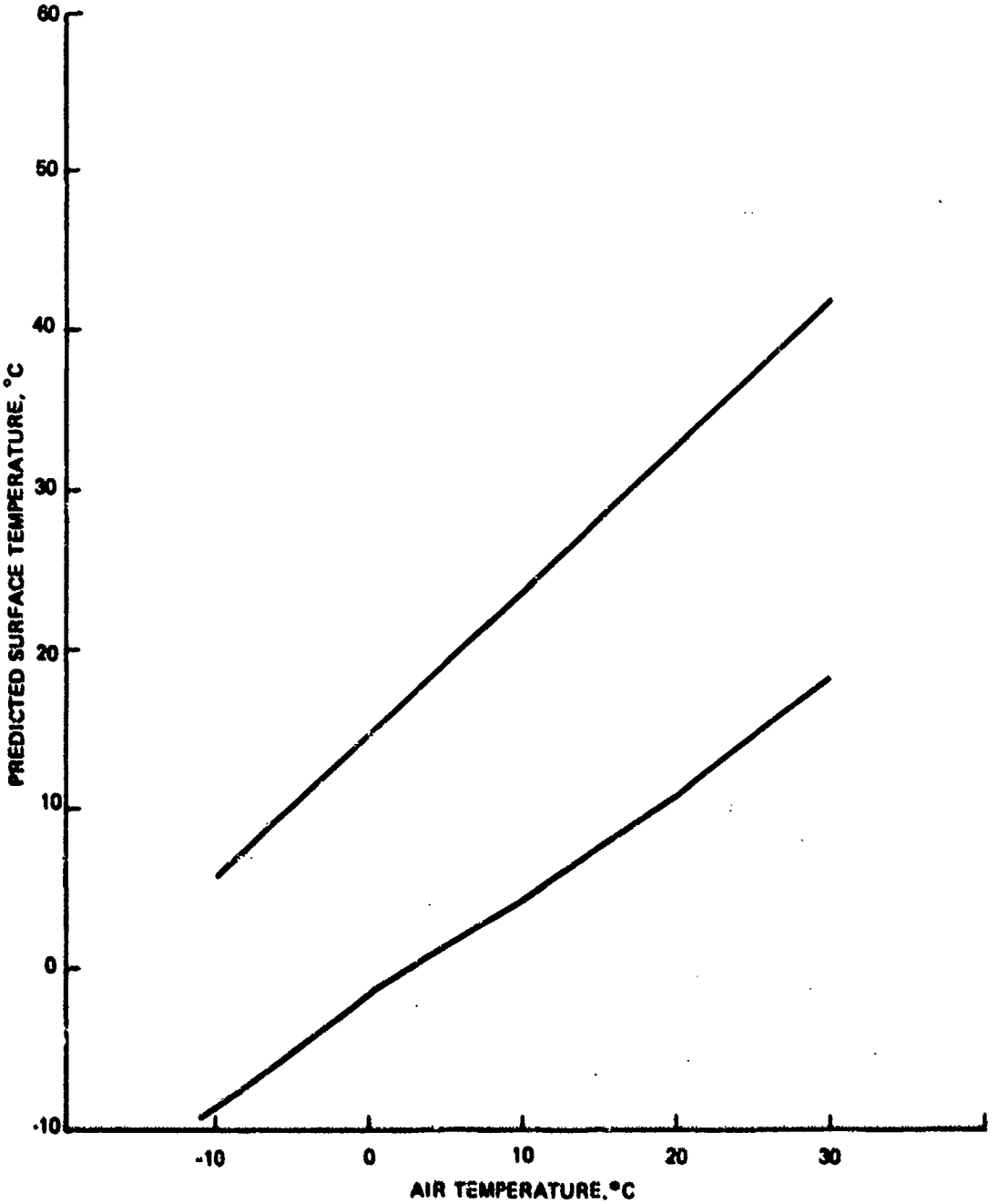

Figure 9. Changes in max-min temperature predictions for variations in air temperature

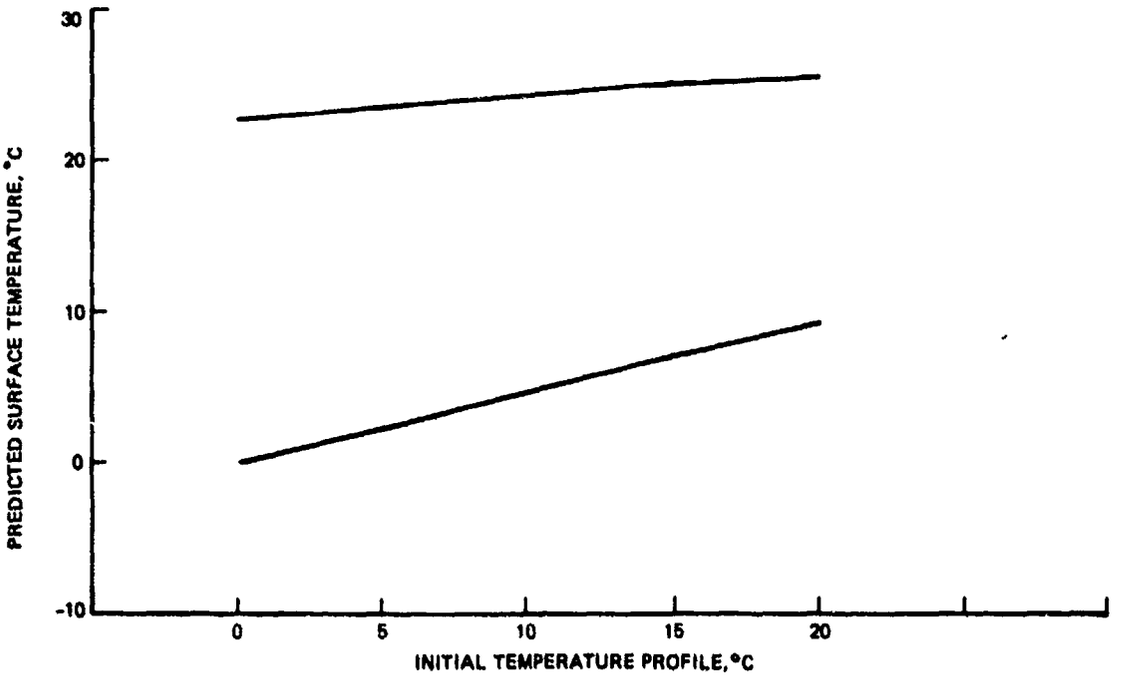

Figure 10. Changes in max-min temperature predictions for variations in the initial temperature profile

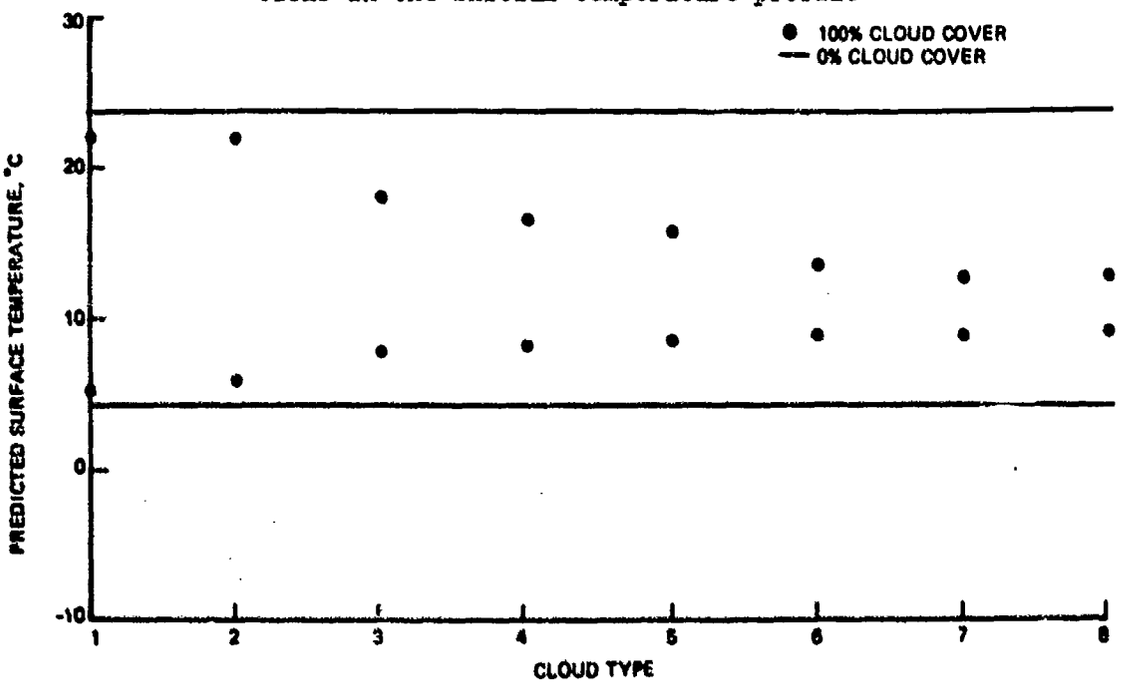

Figure 11. Changes in max-min temperature predictions for variations in cloud type

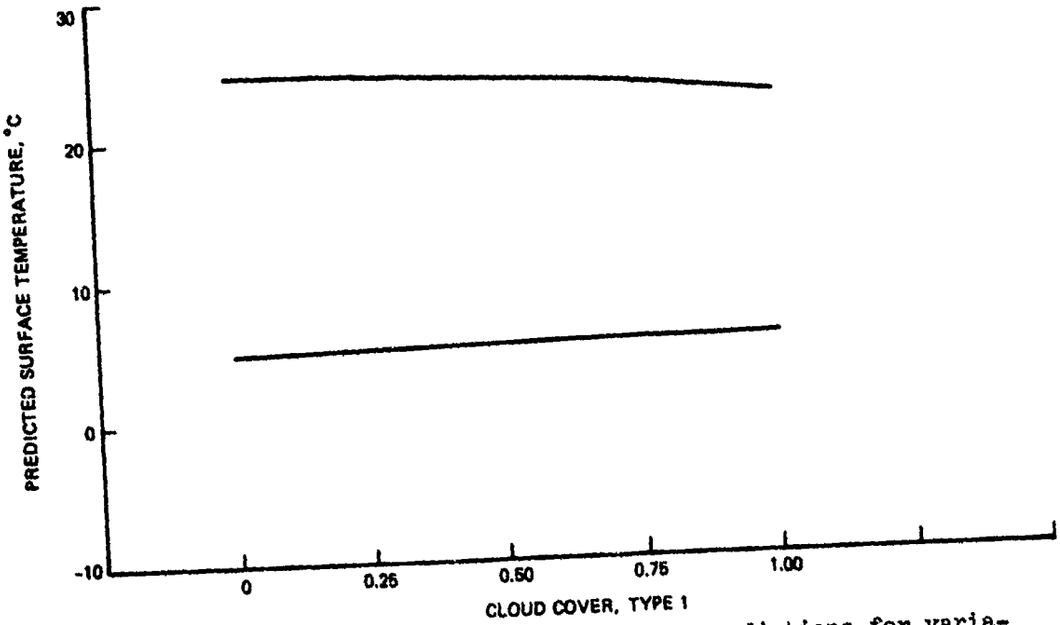

Figure 12. Changes in max-min temperature predictions for variations in cloud cover using cloud type 1

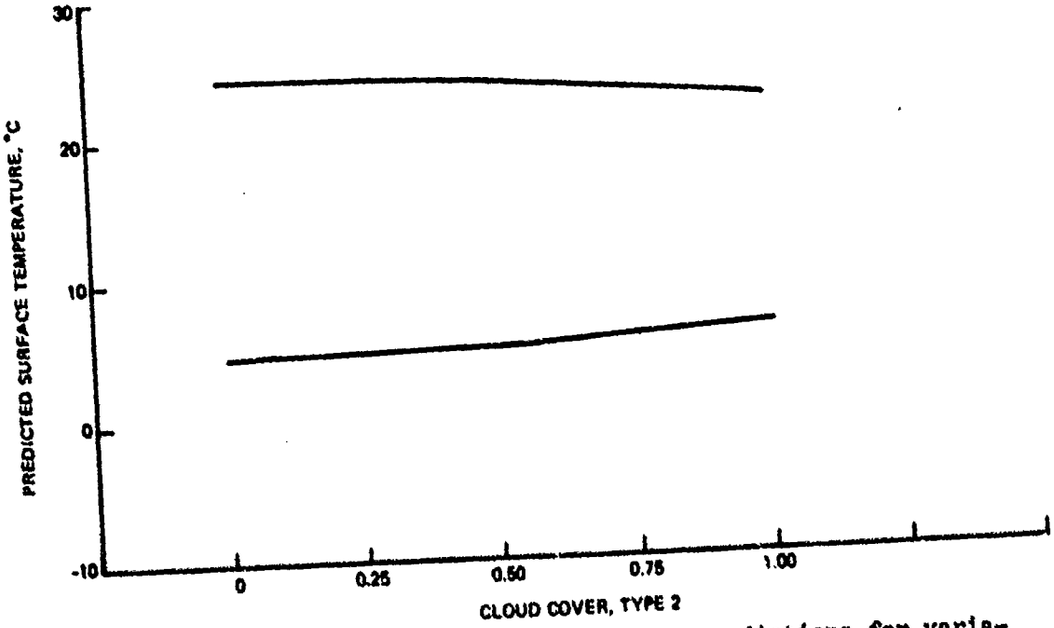

Figure 13. Changes in max-min temperature predictions for variations in cloud cover using cloud type 2

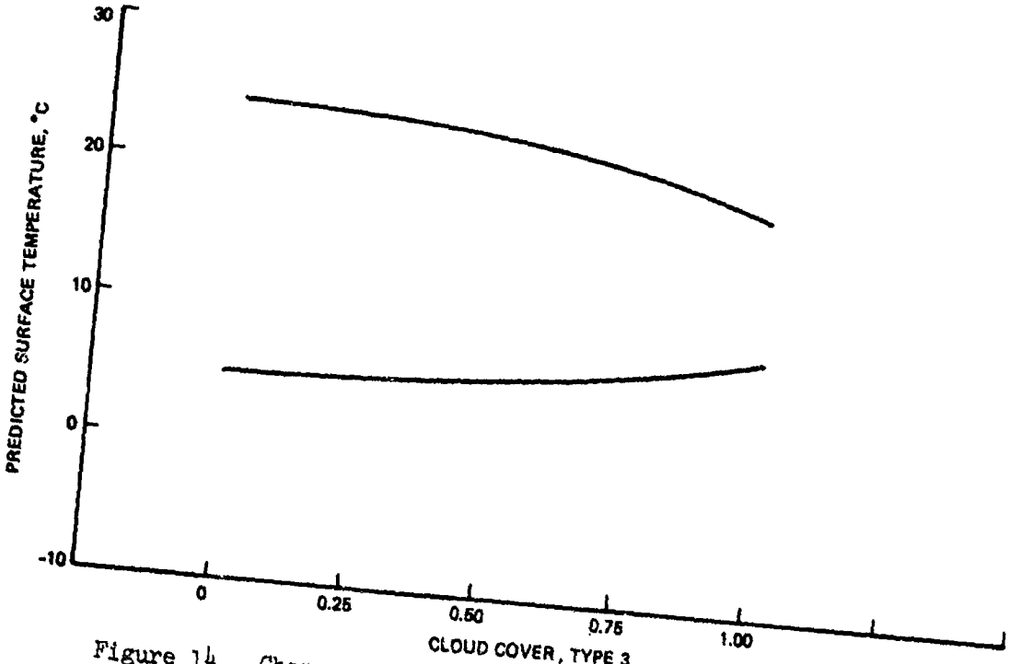

Figure 14. Changes in max-min temperature predictions for variations in cloud cover using cloud type 3

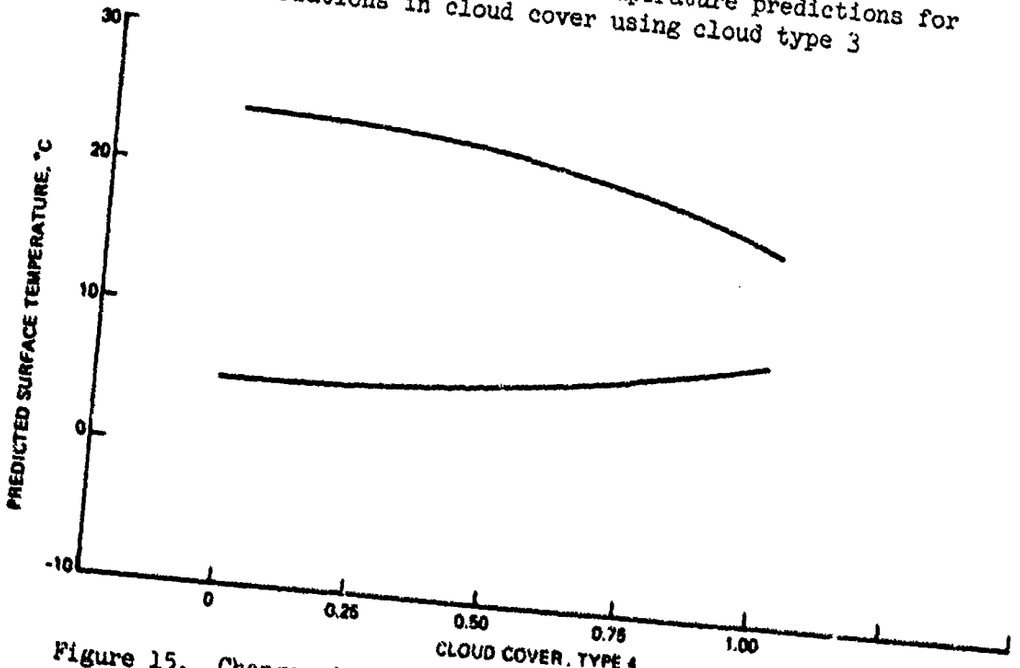

Figure 15. Changes in max-min temperature predictions for variations in cloud cover using cloud type 4

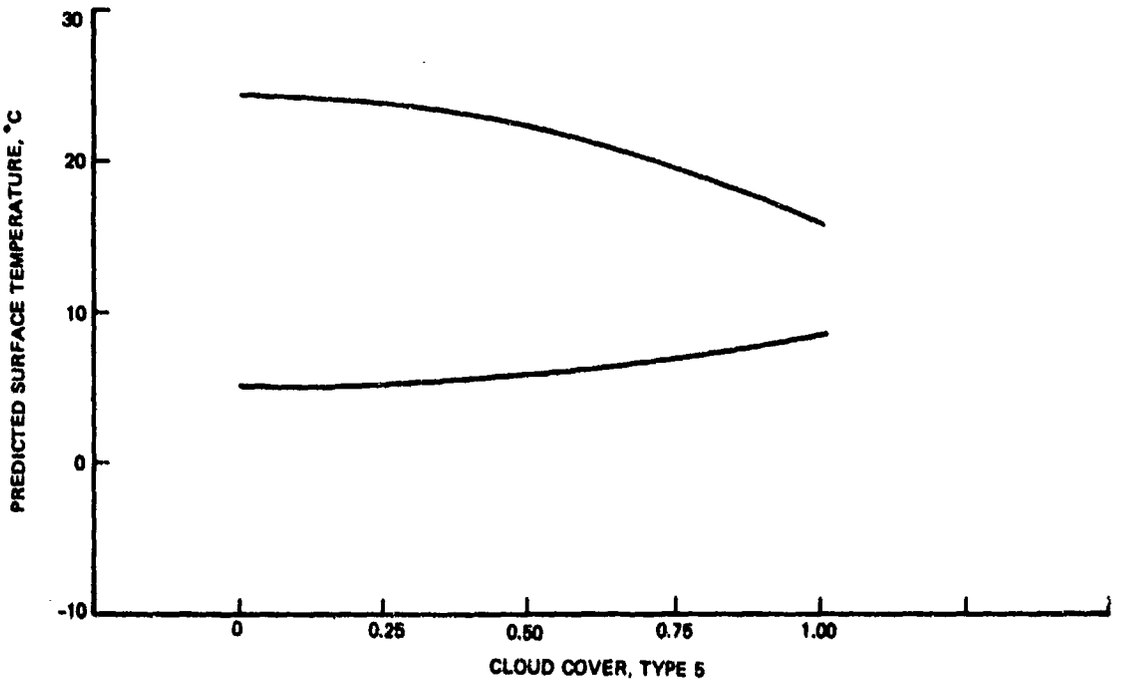

Figure 16. Changes in max-min temperature predictions for variations in cloud cover using cloud type 5

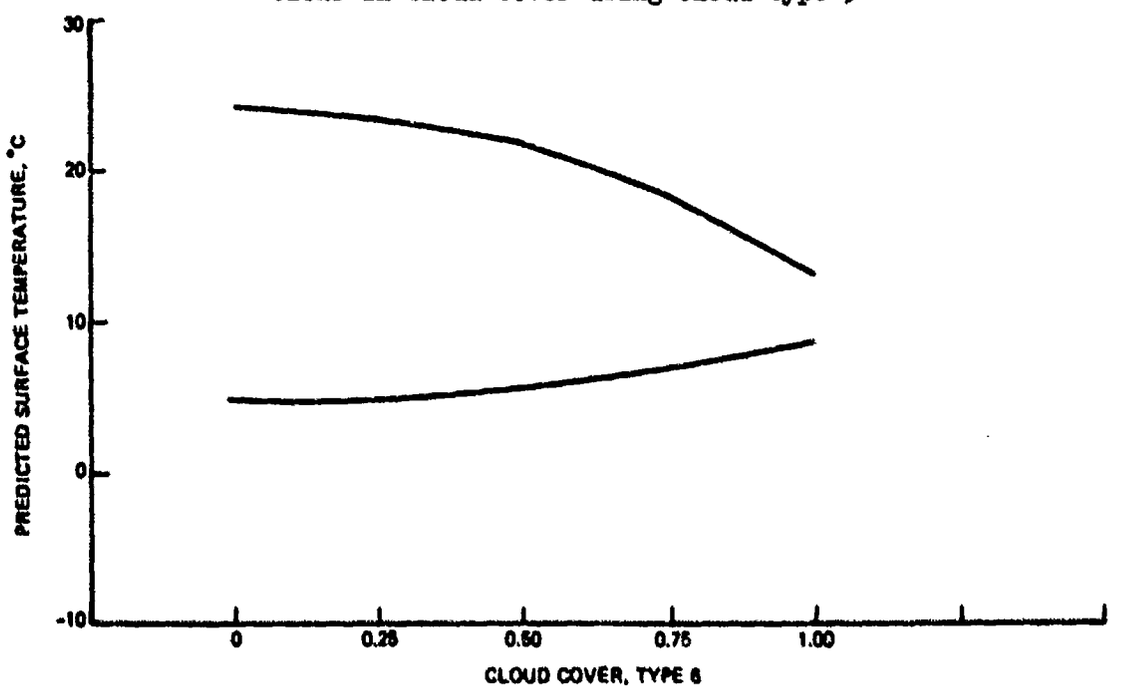

Figure 17. Changes in max-min temperature predictions for variations in cloud cover using cloud type 6

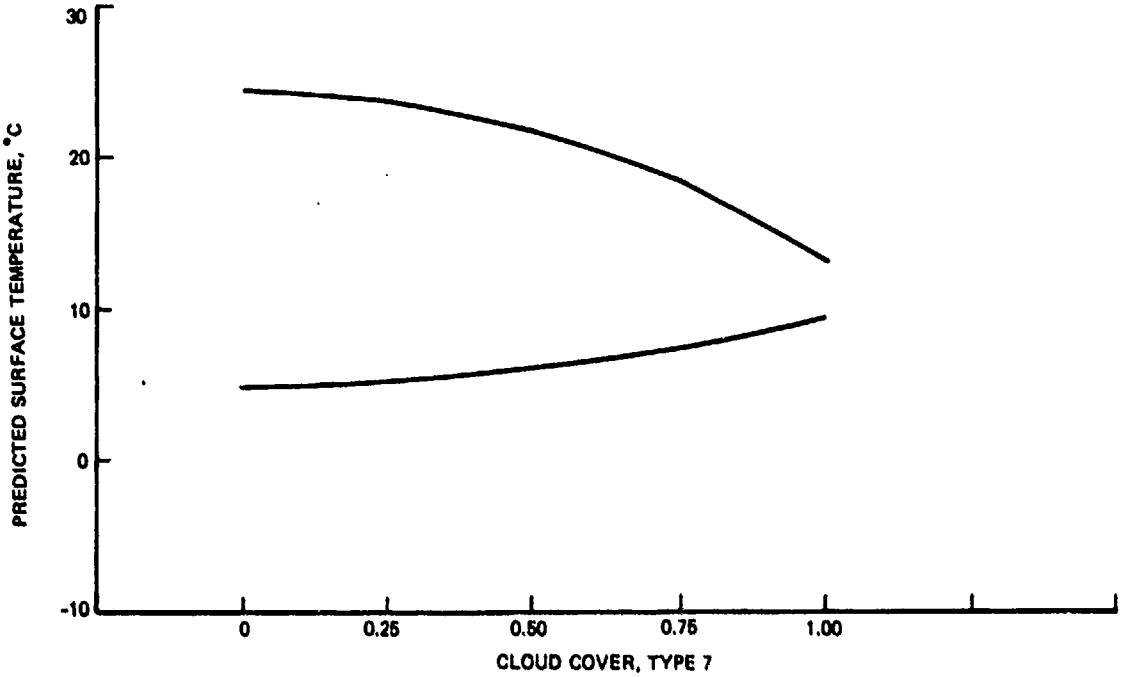

Figure 18. Changes in max-min temperature predictions for variations in cloud cover using cloud type 7

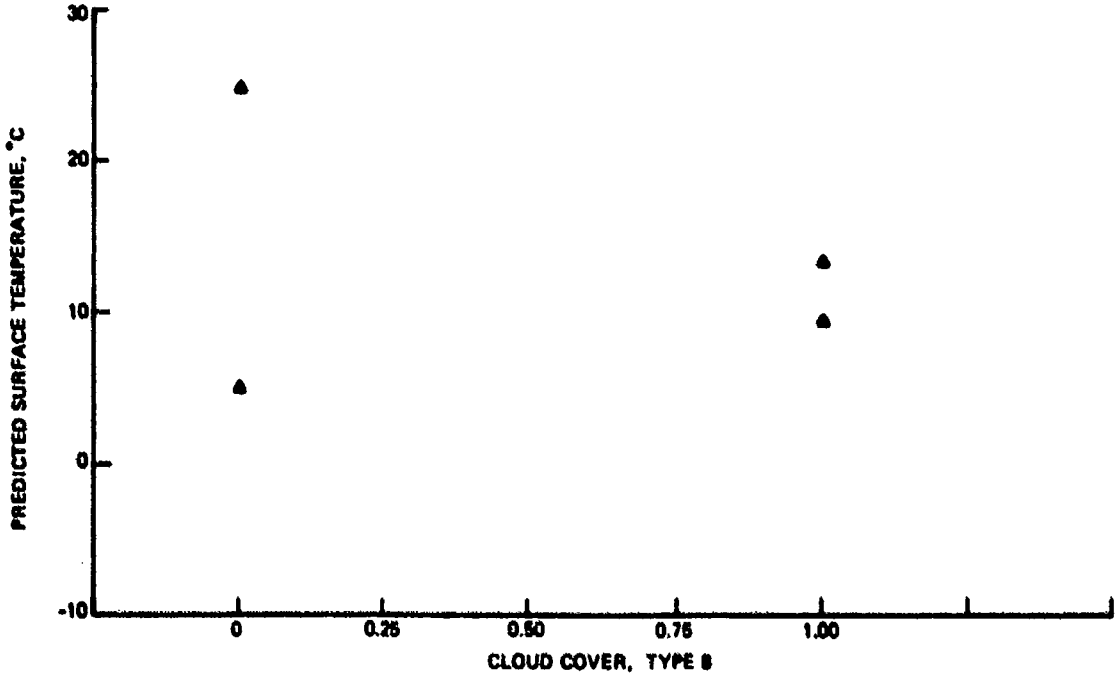

Figure 19. Changes in max-min temperature predictions for variations in cloud cover using cloud type 8

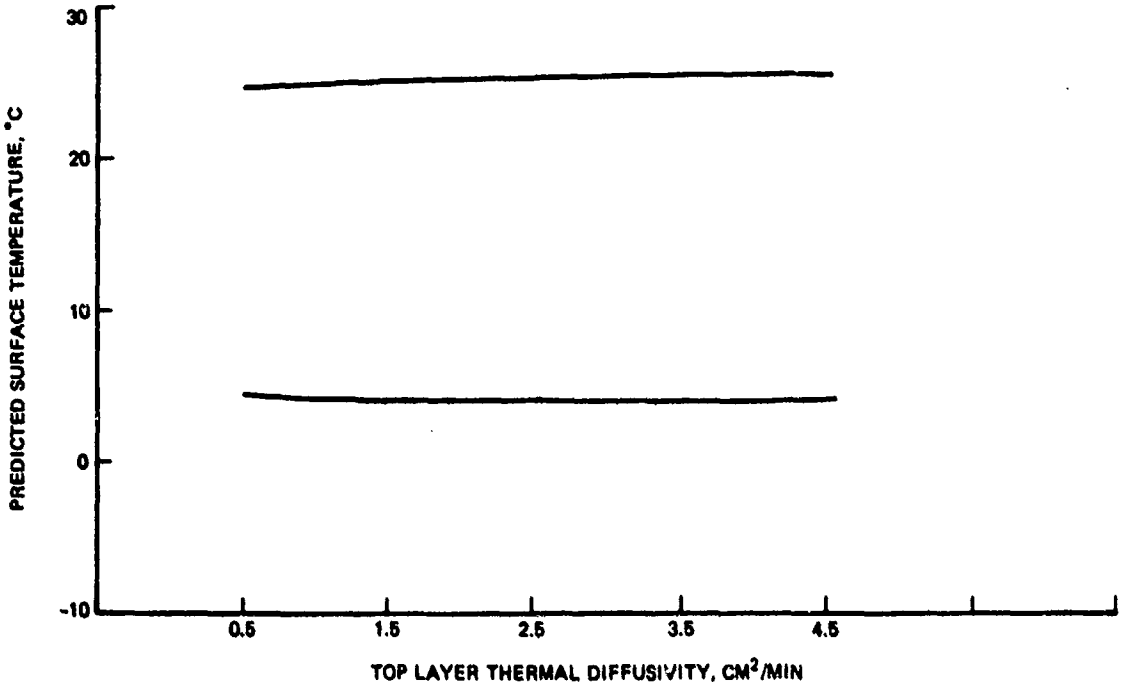

Figure 20. Changes in max-min temperature predictions for variations in thermal diffusivity

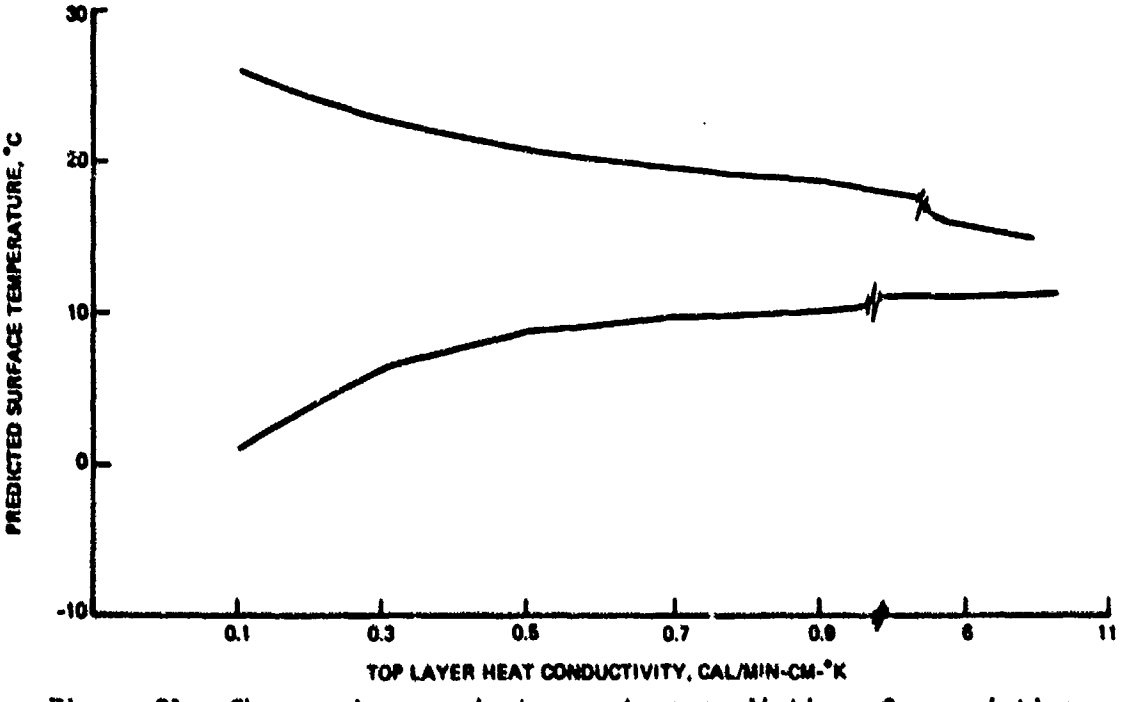

Figure 21. Changes in max-min temperature predictions for variations in heat conductivity

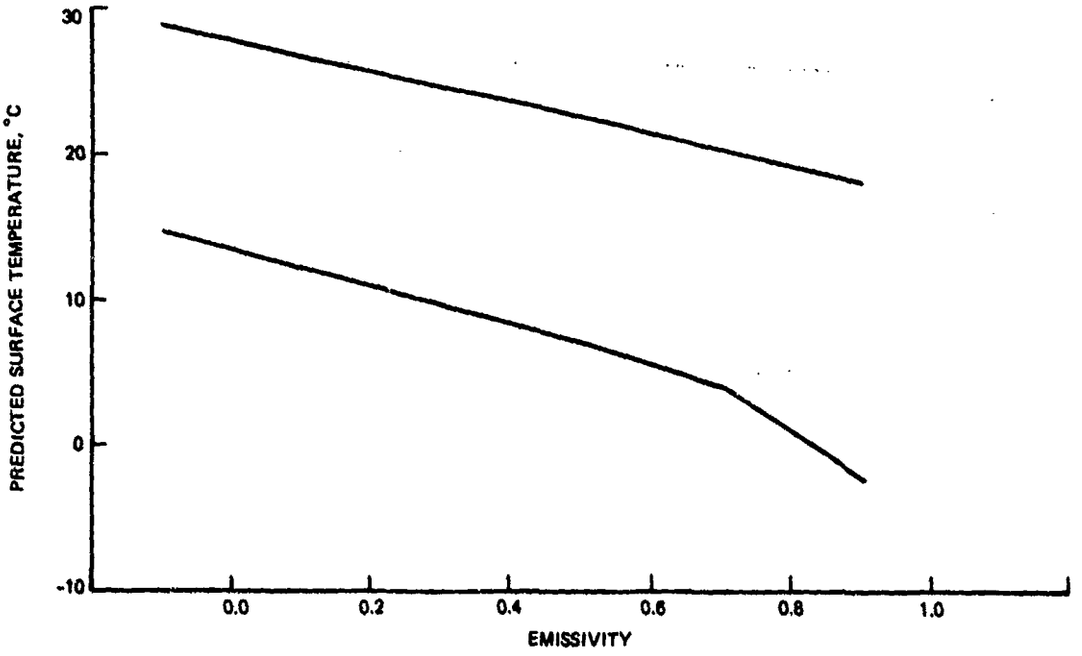

Figure 22. Changes in max-min temperature predictions for variations in longwave emissivity

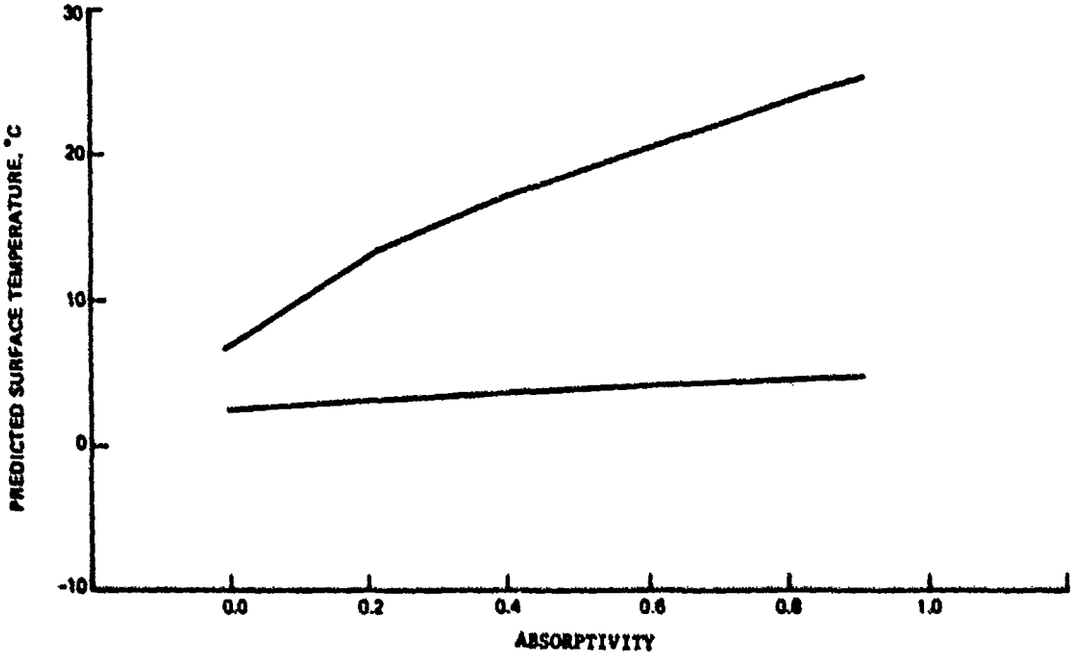

Figure 23. Changes in max-min temperature predictions for variations in shortwave absorptivity

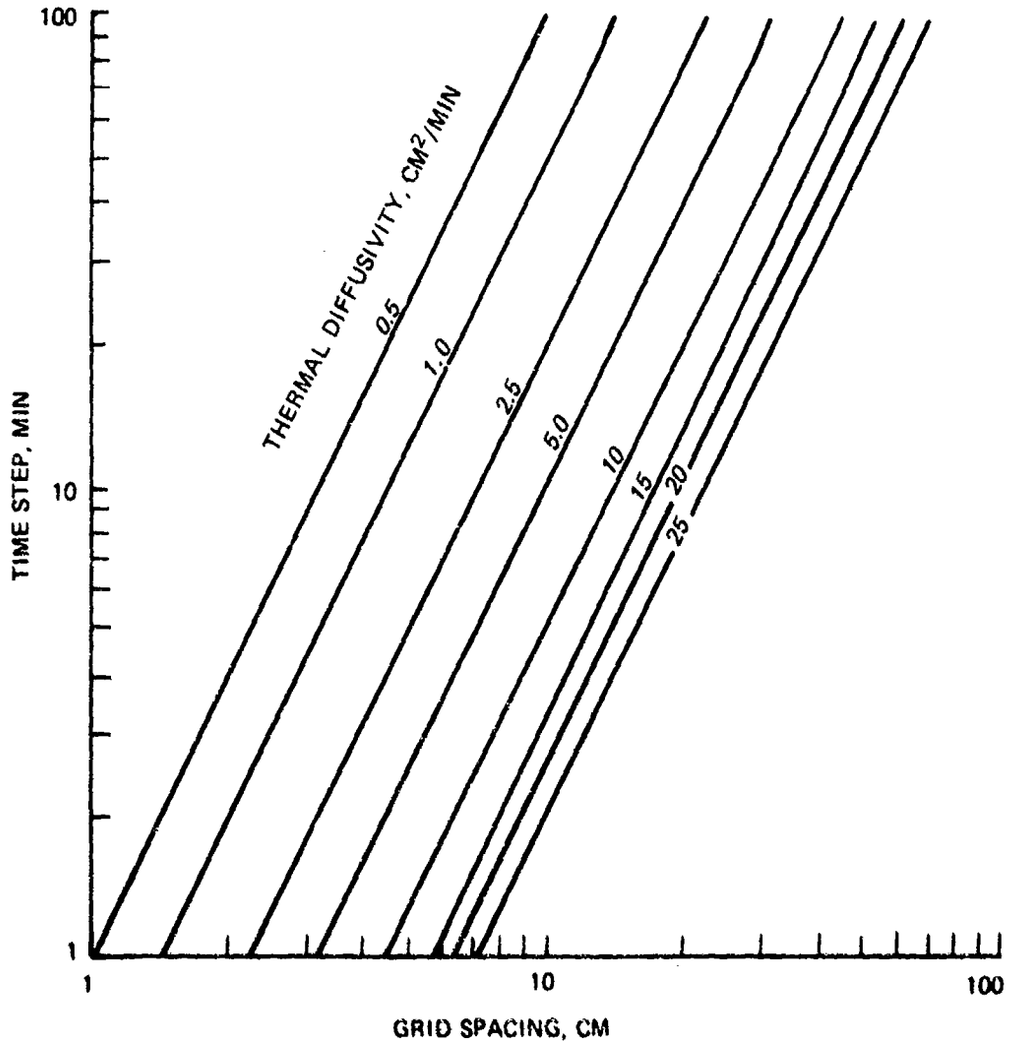

Figure 24. Grid spacing-time step relation for different thermal diffusivities to ensure numerical stability

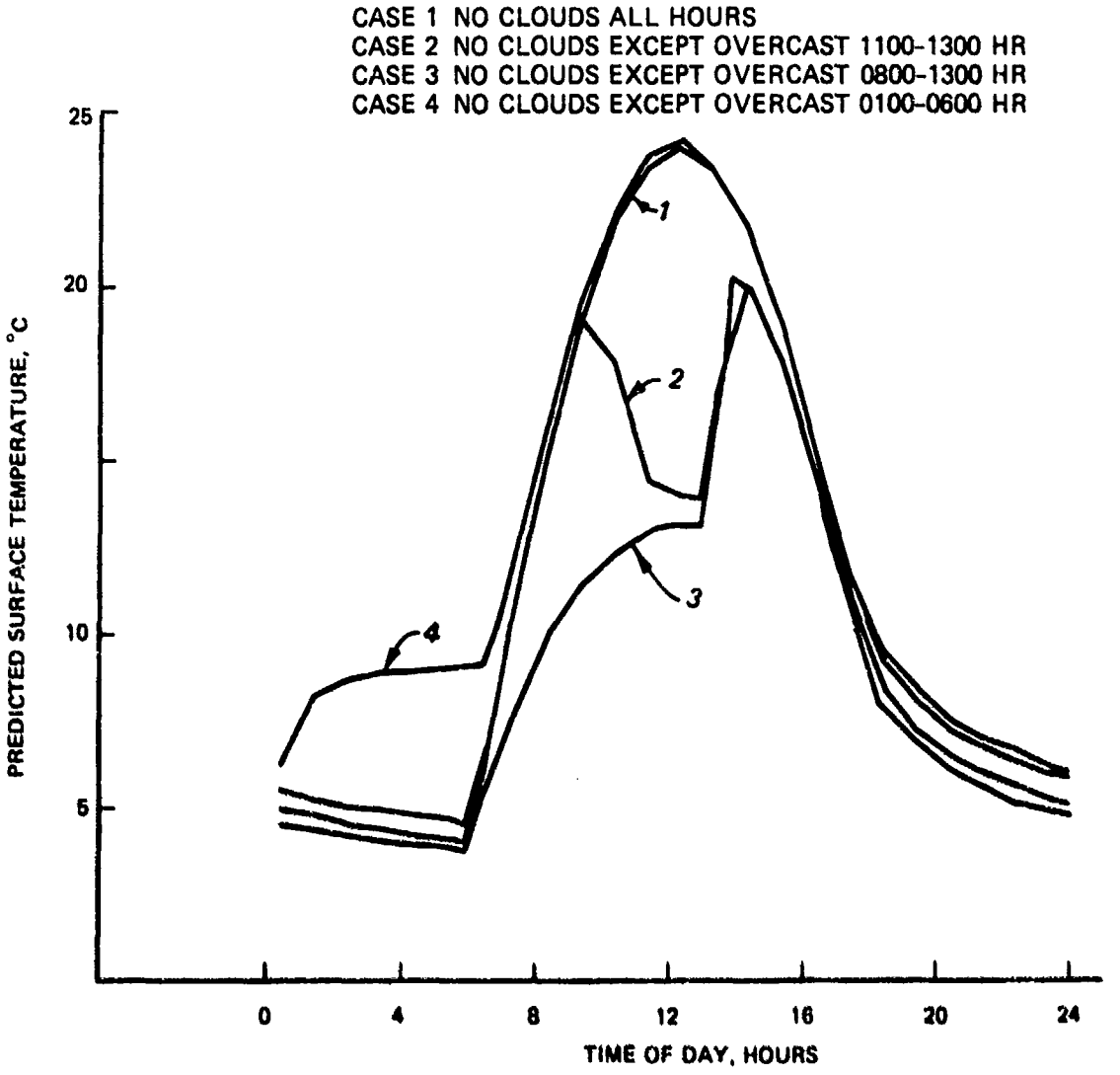

Figure 25. Model predictions for different diurnal cloud cover profiles, base cloud cover of 0 percent

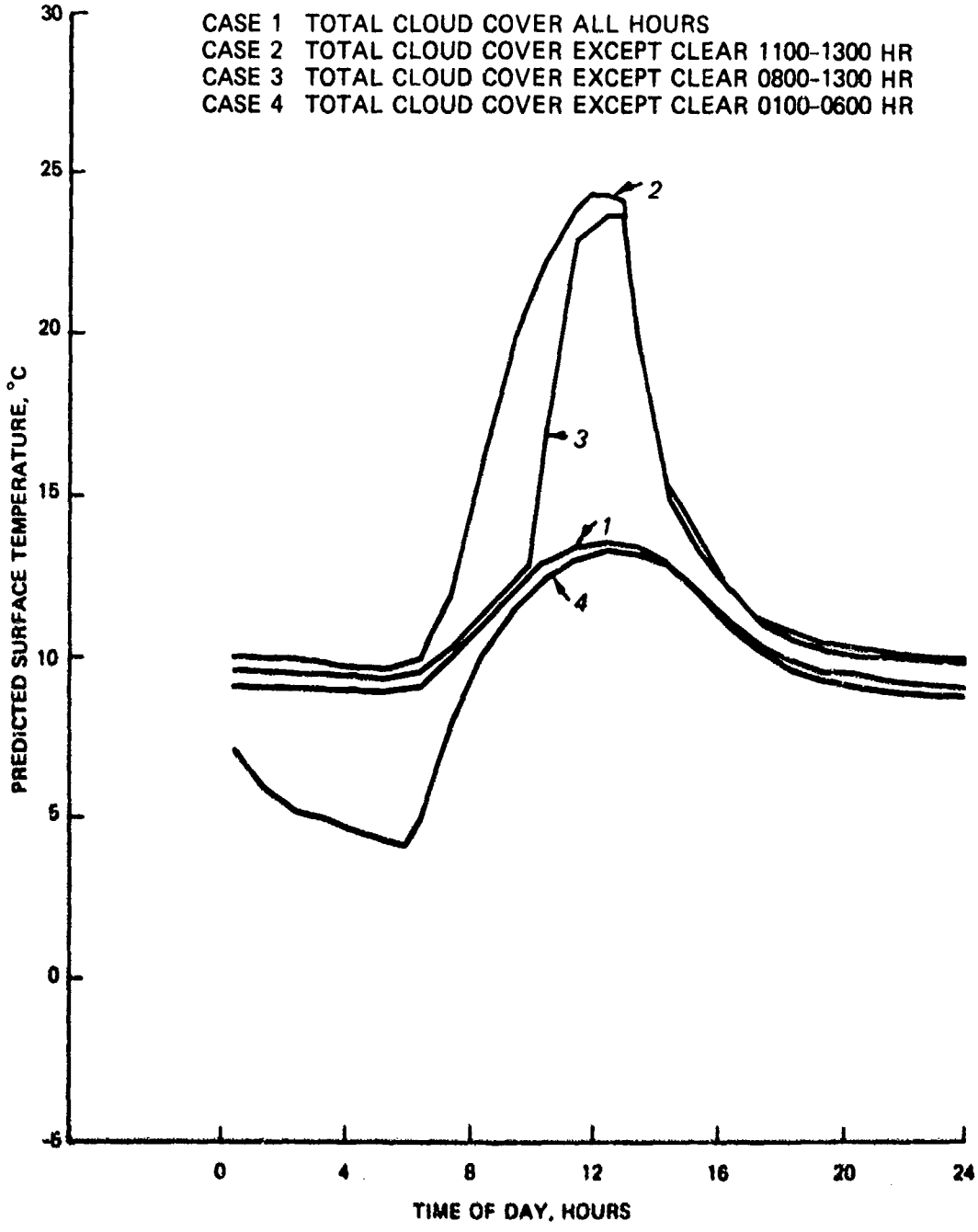

Figure 26. Model predictions for different diurnal cloud cover profiles, base cloud cover of 100 percent

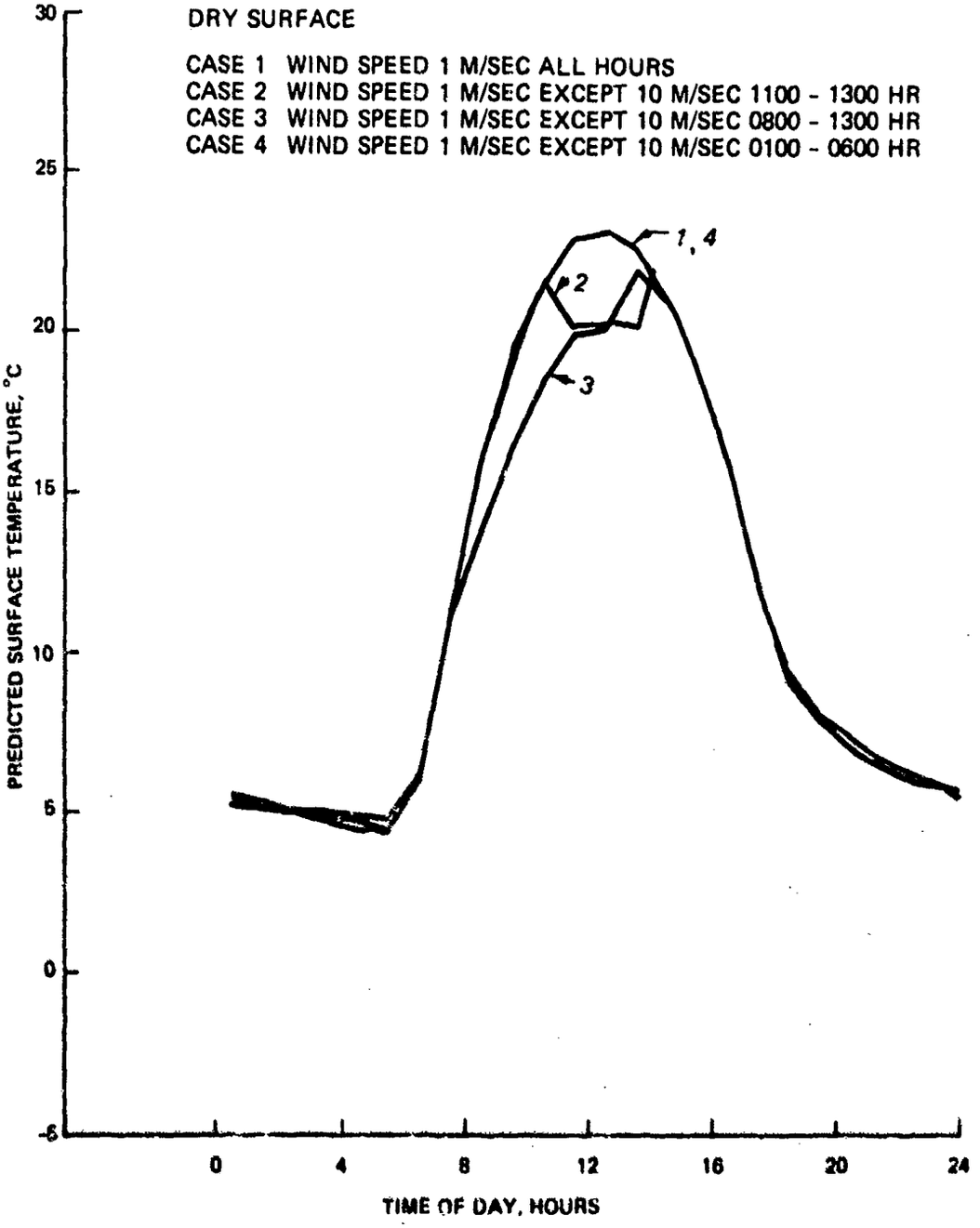

Figure 27. Model predictions for different diurnal wind speed profiles, dry surface

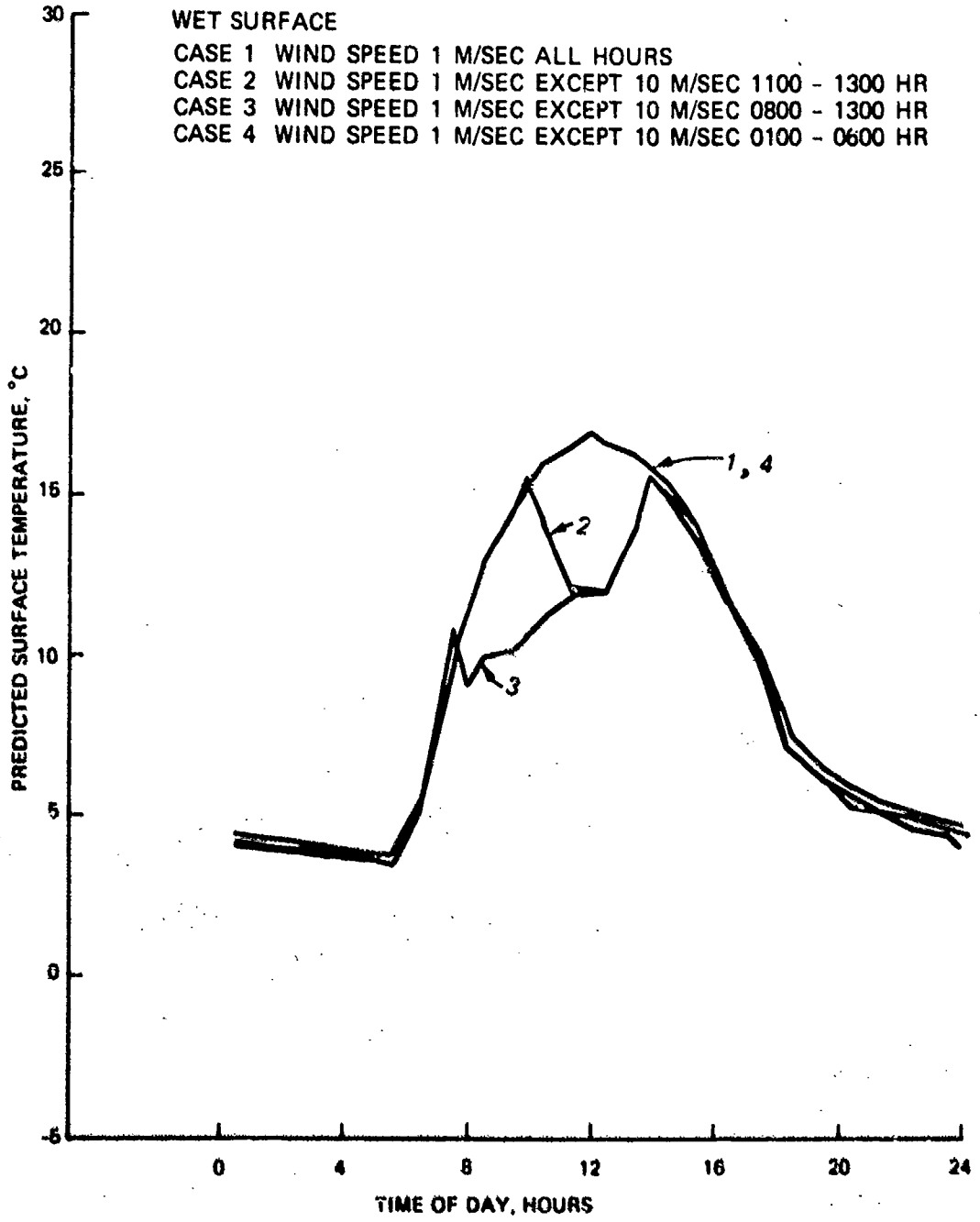

Figure 28. Model predictions for different diurnal wind speed profiles, saturated surface

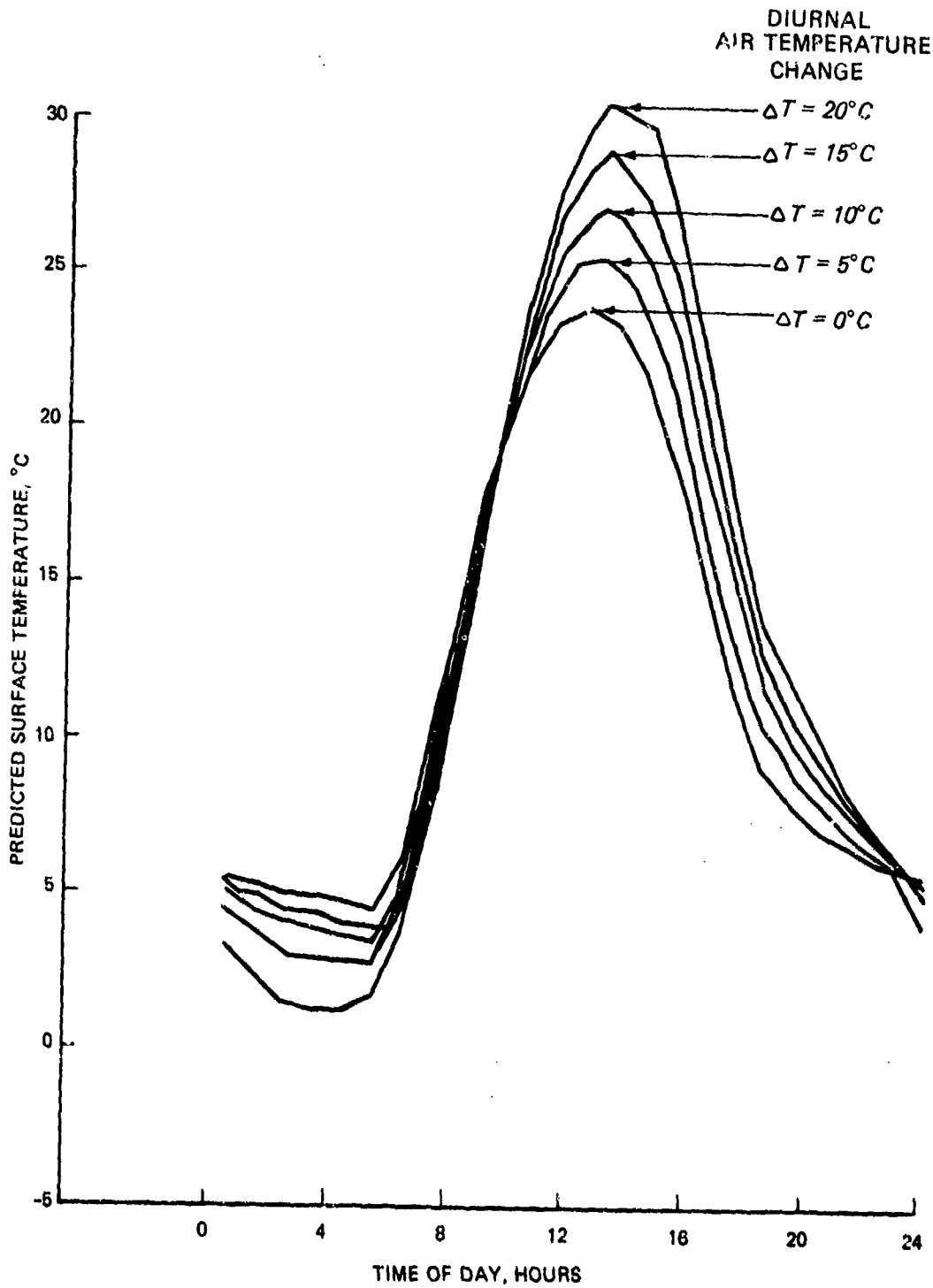

Figure 29. Model predictions for different diurnal air temperature profiles

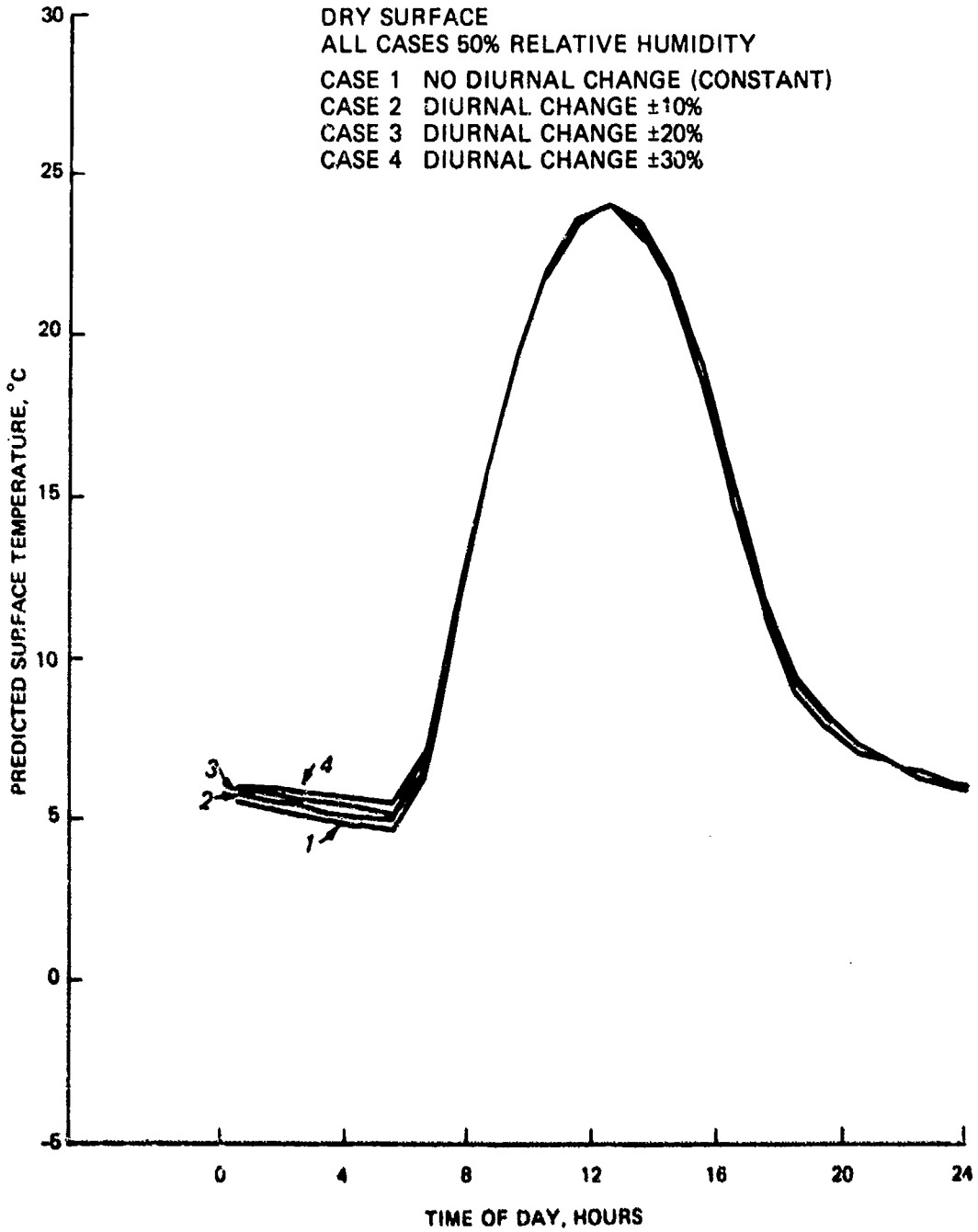

Figure 30. Model predictions for different diurnal relative humidity profiles, dry surface

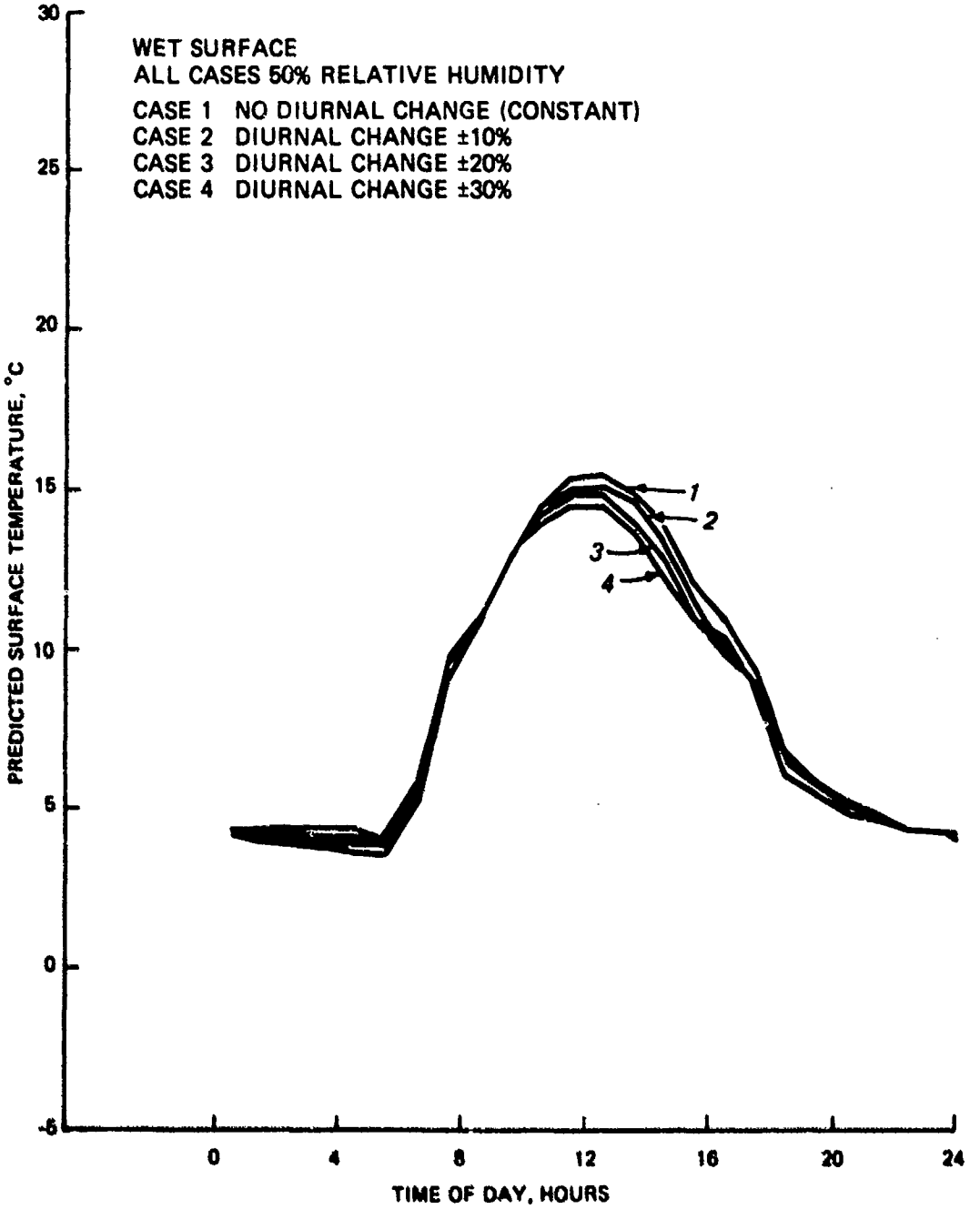

Figure 31. Model predictions for different diurnal relative humidity profiles, saturated surface

ATMOSPHERIC-SPECIFICATIONS

ATMOS PRESS MB	CLOUD TYPE INDEX	SHELTER HEIGHT-CM
1000.0	1	200.00

TIME HR	AIR TEMP DEG C	RH %	CLOUD COVER (0-1)	WIND SPEED M/SEC
0.	10.0	50.0	0.	4.4
1.0	10.0	50.0	0.	4.4
2.0	10.0	50.0	0.	4.4
3.0	10.0	50.0	0.	4.4
4.0	10.0	50.0	0.	4.4
5.0	10.0	50.0	0.	4.4
6.0	10.0	50.0	0.	4.4
7.0	10.0	50.0	0.	4.4
8.0	10.0	50.0	0.	4.4
9.0	10.0	50.0	0.	4.4
10.0	10.0	50.0	0.	4.4
11.0	10.0	50.0	0.	4.4
12.0	10.0	50.0	0.	4.4
13.0	10.0	50.0	0.	4.4
14.0	10.0	50.0	0.	4.4
15.0	10.0	50.0	0.	4.4
16.0	10.0	50.0	0.	4.4
17.0	10.0	50.0	0.	4.4
18.0	10.0	50.0	0.	4.4
19.0	10.0	50.0	0.	4.4
20.0	10.0	50.0	0.	4.4
21.0	10.0	50.0	0.	4.4
22.0	10.0	50.0	0.	4.4
23.0	10.0	50.0	0.	4.4
24.0	10.0	50.0	0.	4.4

SURFACE-ORIENTATION-SPECIFICATIONS

SFC SLOPE DEG-HORIZ = 0	SFC AZIMUTH DEG S=0	DAY JULIAN	LATITUDE DEG
0.	0.	91.0	45.0

HEAT-FLOW-CALCULATION-CONTROLS

NO. OF LAYERS	NO. OF 24 HR REPETITIONS	TIME STEP MIN	PRINT FREQ MIN
1-6			
3	4.0	15.	30.

NUMBER OF PROFILE POINTS = 5

DEPTH CM	TEMP DEG C
0.	10.0
15.0	10.0
45.0	10.0
100.0	10.0
145.0	10.0

TOP-SURFACE-CONSTANTS

EMISS	ABSORP	SATURATION
0.95	0.92	0.0

INPUT-LAYER-SPECIFICATIONS

LAYER NO.	THICKNESS CM	VERT. GRID SPACE-CM	THERMAL DIFF CM**2/MIN	HEAT COND CAL/MIN-CM-K
1	15.0	5.0	0.30	0.30
2	30.0	10.0	0.10	0.60
3	100.0	10.0	0.40	0.30

INPUT BOTTOM BOUNDARY DATA

BOTTOM BOUNDARY INDEX = 0
BOTTOM BOUNDARY TEMPERATURE = 10.0 DEG C

Figure 32. Standard day used for sensitivity analysis

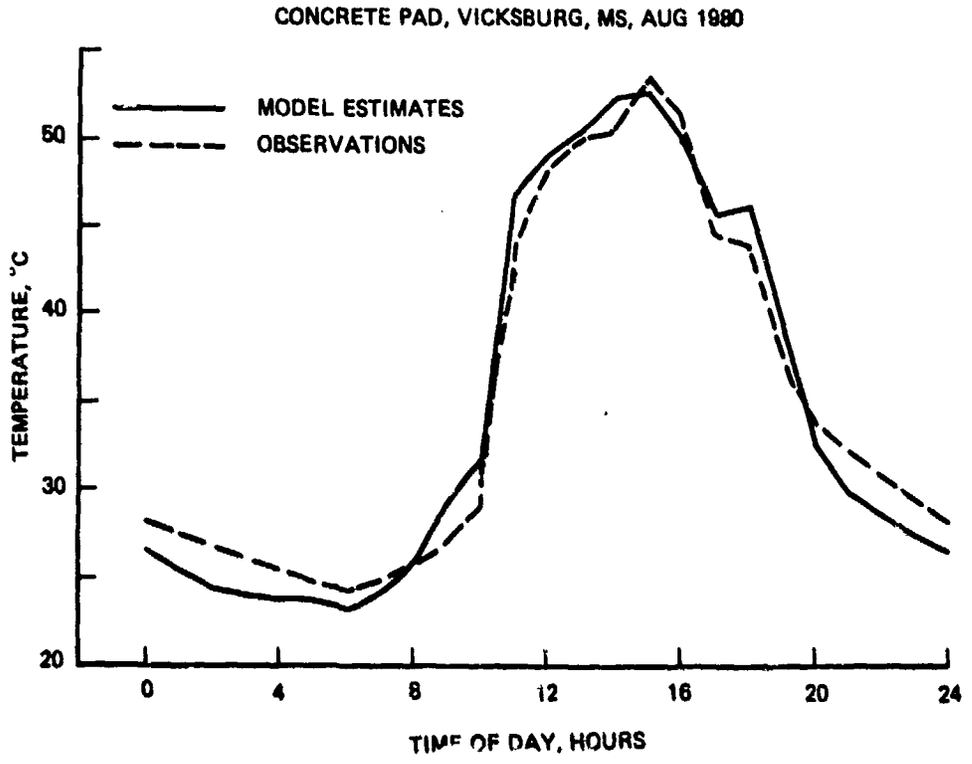

Figure 33. Predicted and measured temperatures for concrete pad

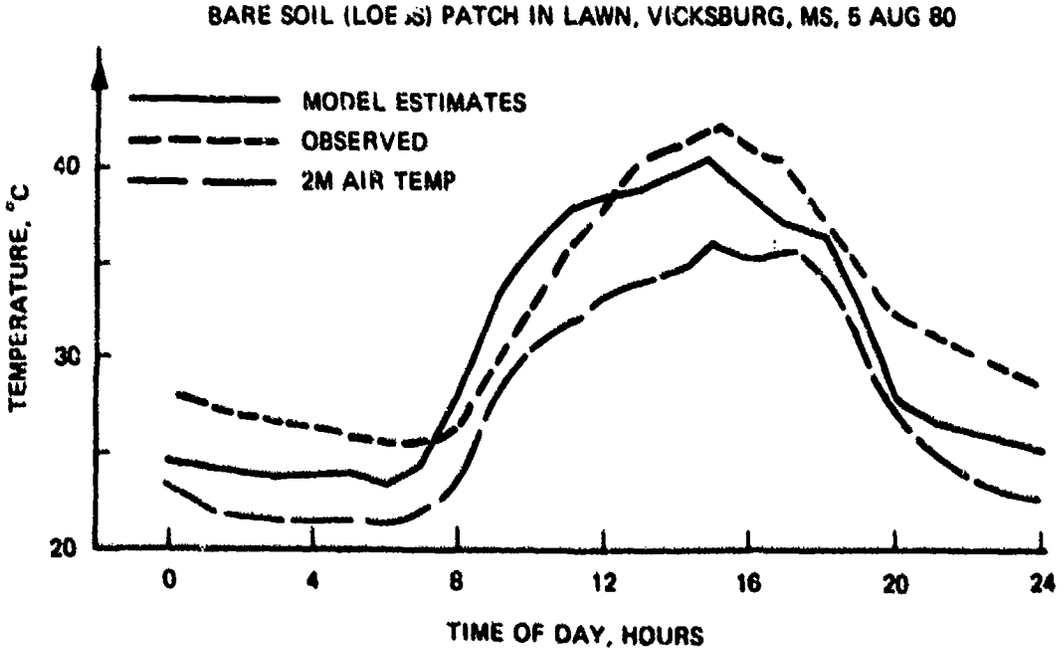

Figure 34. Predicted and measured temperatures for bare soil, 5 August 1980

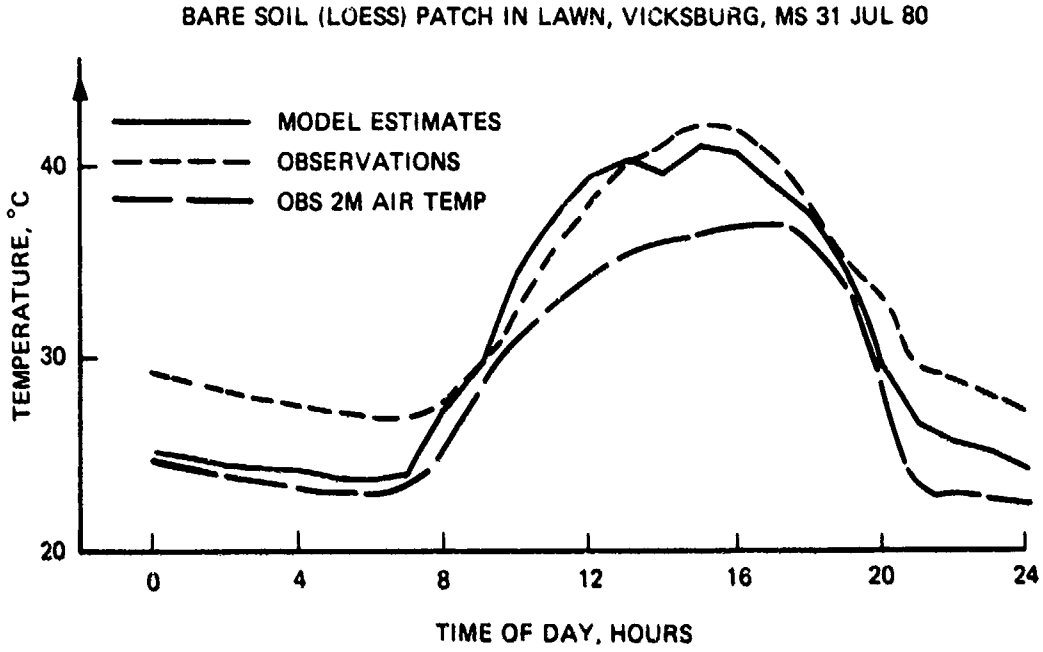

Figure 35. Predicted and measured temperatures for bare soil, 31 July 80

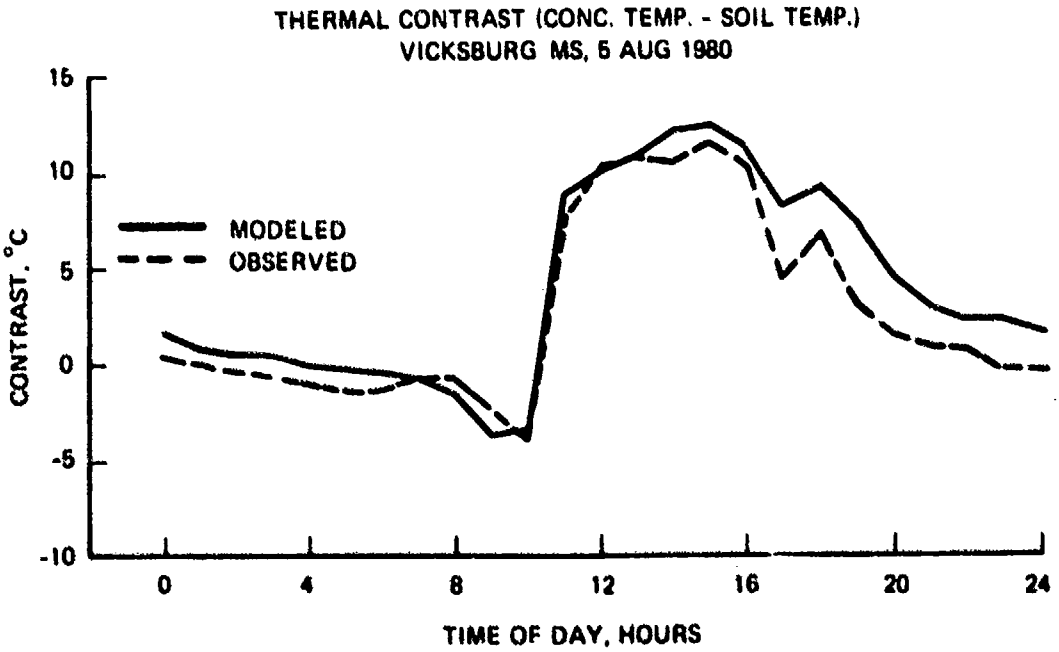

Figure 36. Predicted and measured thermal contrast for concrete pad and bare soil

APPENDIX A: SIMPLIFIED FLOWCHART AND VARIABLE DEFINITIONS

1. The logic of the TSTM computer code is of such complexity (a computer-generated flowchart requires 52 pages) that a simplified flowchart was deemed of more benefit in providing the user an understanding of the organization of the computer code.

2. The flowchart presented in Figure A1 avoids the many "counters," such as those found in the location of node points and layers, time print frequency, and interpolation procedures, in the program. It should be noted that the boundary conditions are calculated at each time increment; thus, each of the energy components as discussed in Part II is recalculated. In employing the Newton-Raphson scheme at both the upper and lower boundaries, the energy components are also recalculated, with the last estimate of the appropriate temperature, for each iteration involved in obtaining the top surface temperature and the temperature of the bottom surface.

3. The flowchart is followed by Table A1, which gives definitions of the major variables used in the computer code.

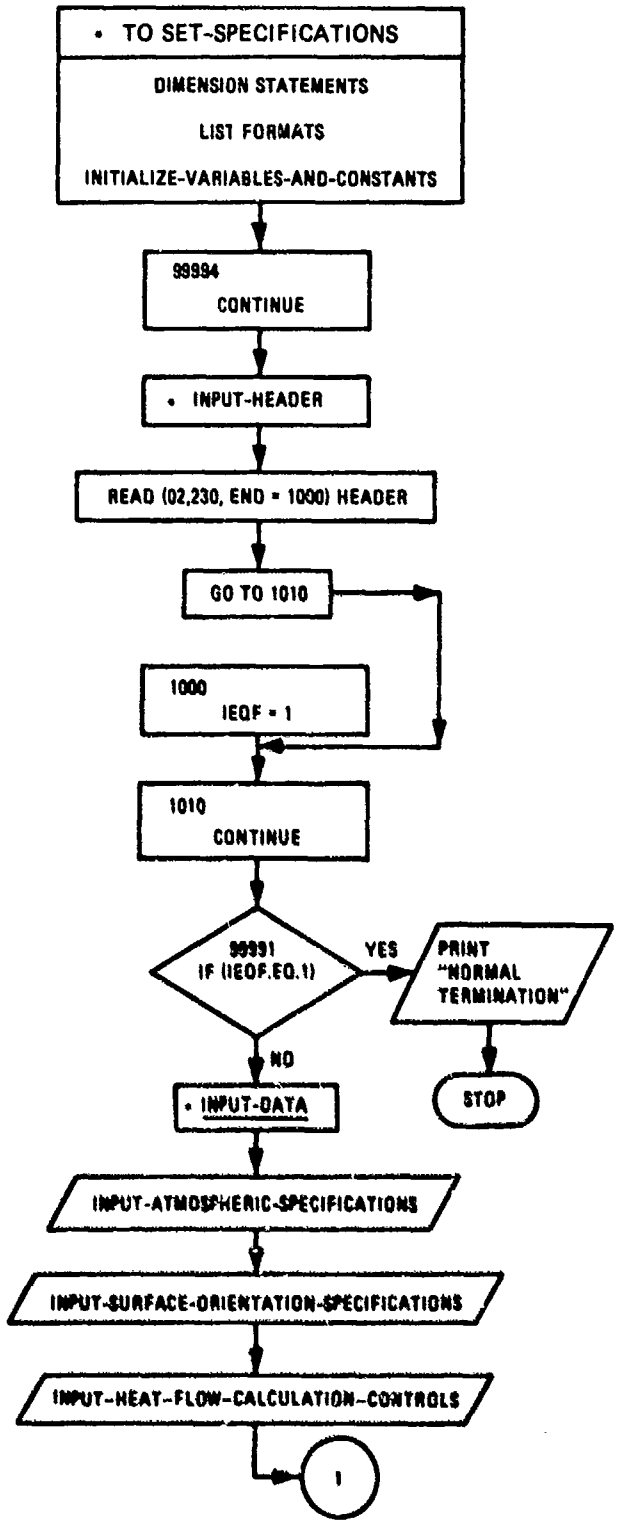

Figure A1. Simplified flowchart for TSTM
(Sheet 1 of 5)

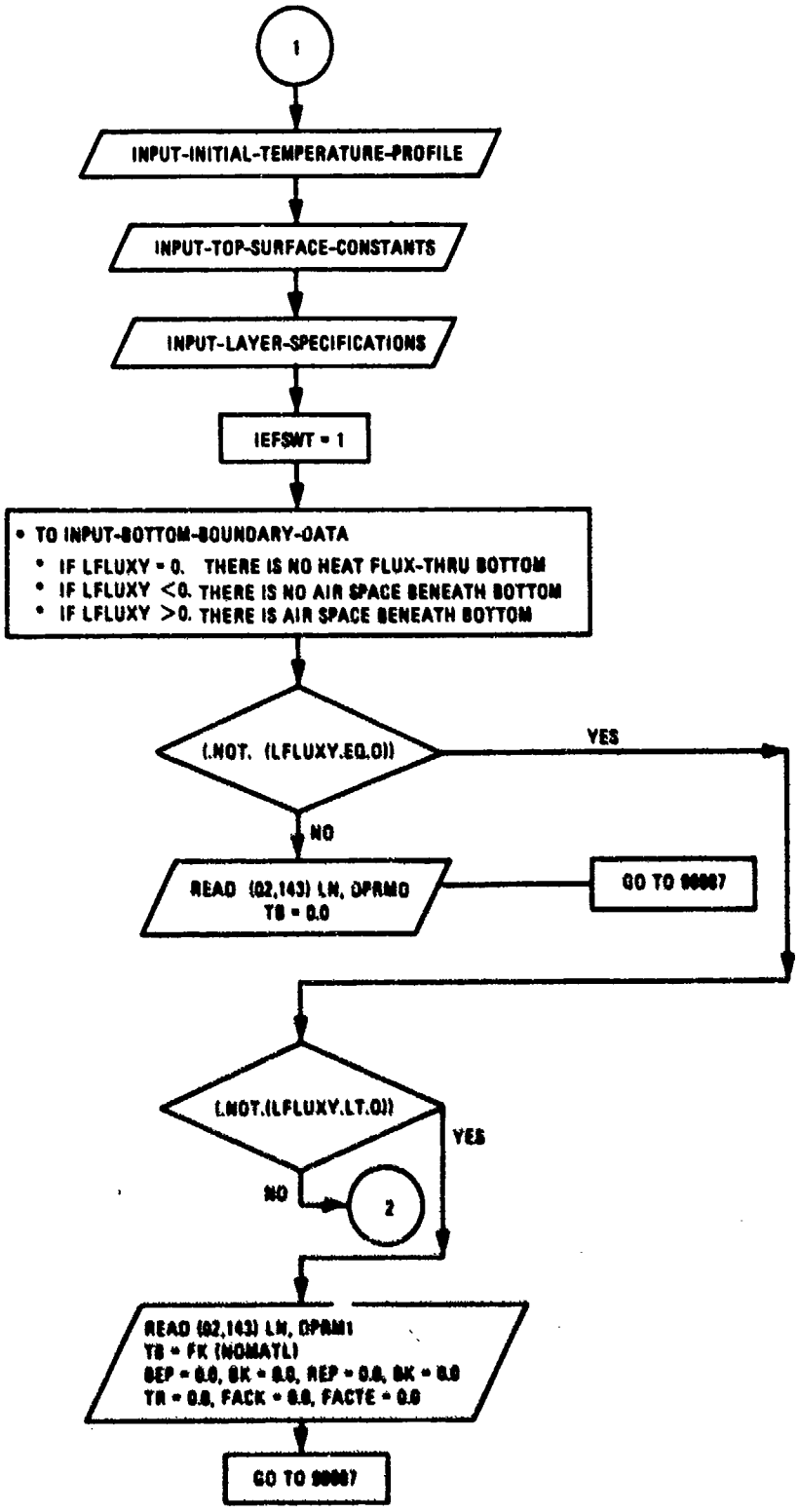

Figure A1. (Sheet 2 of 5)

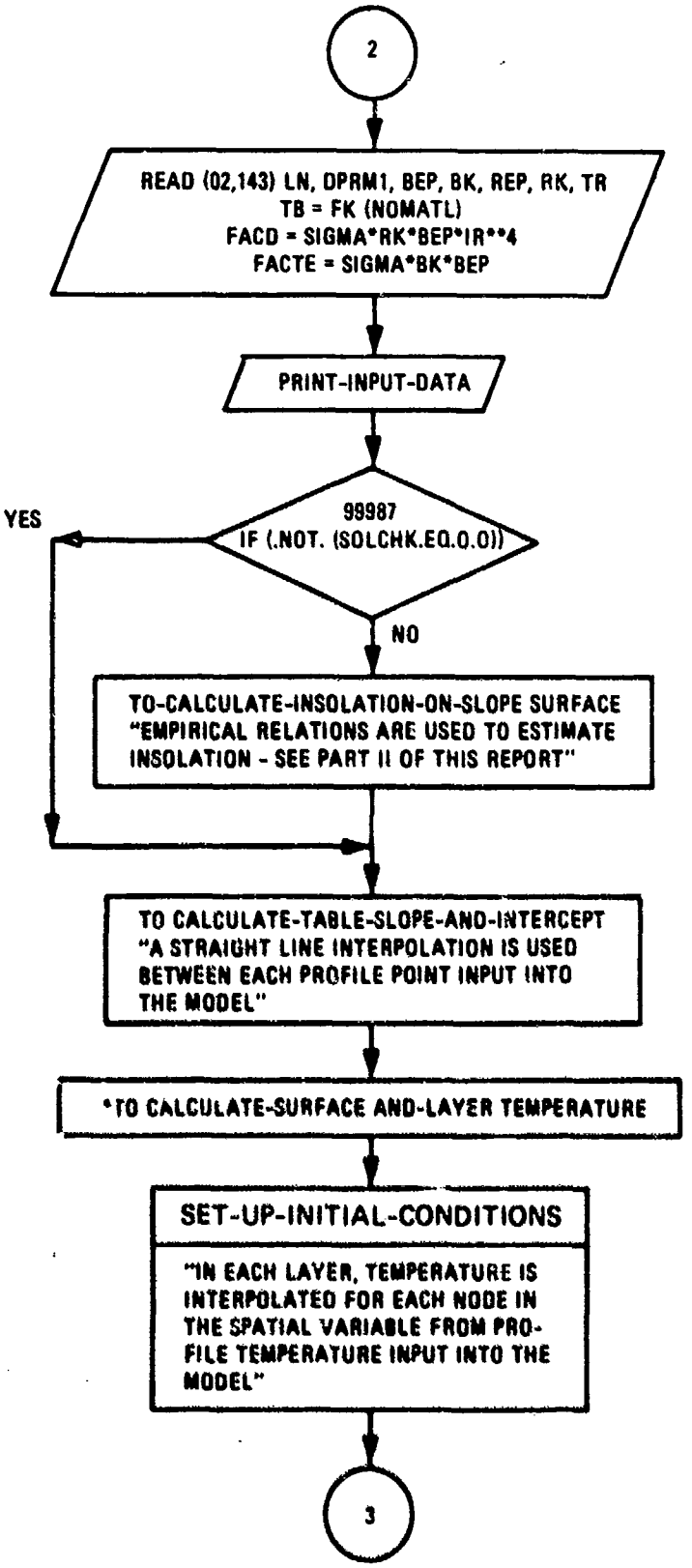

Figure A1. (Sheet 3 of 5)

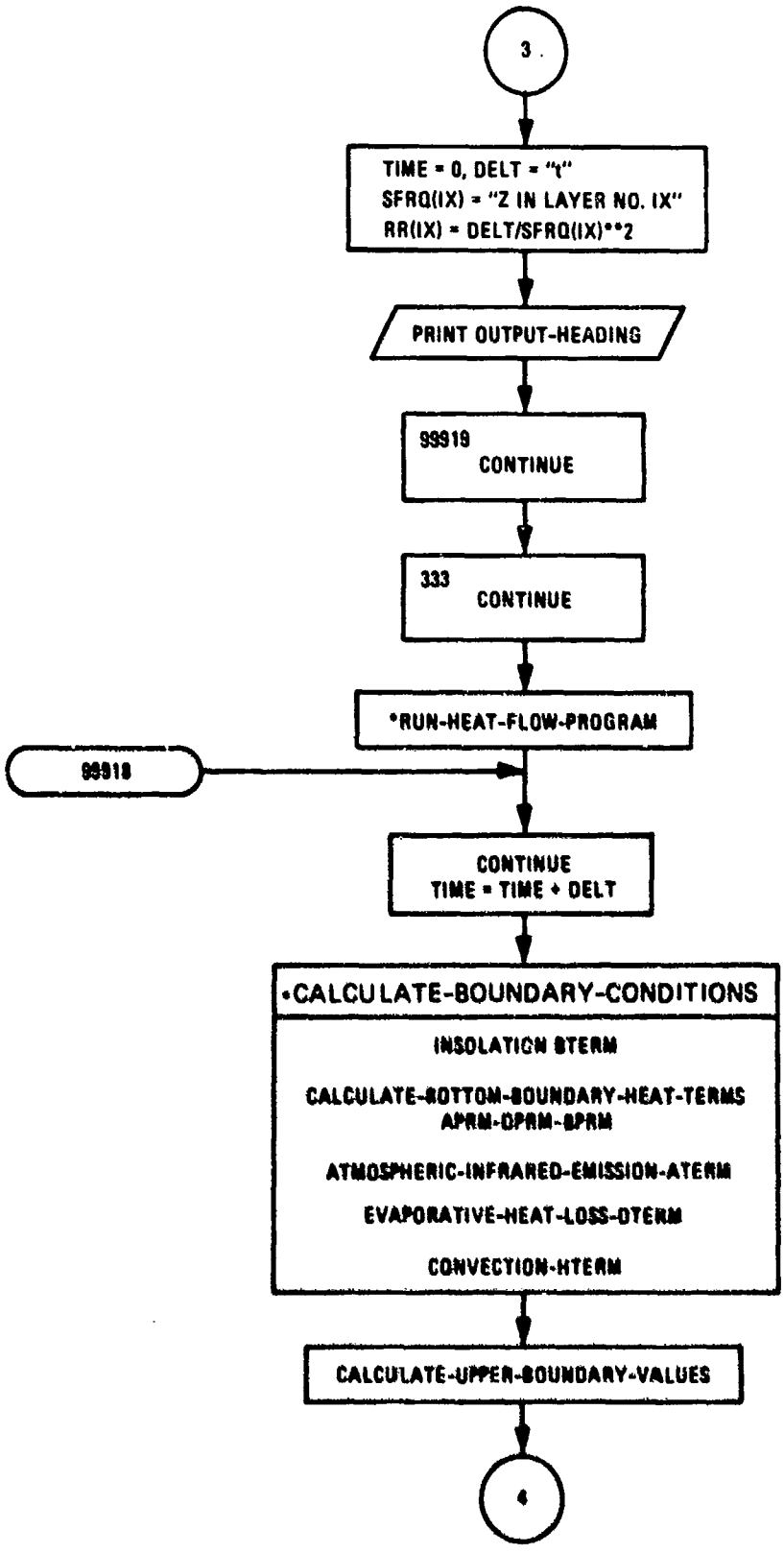

Figure A1. (Sheet 4 of 5)

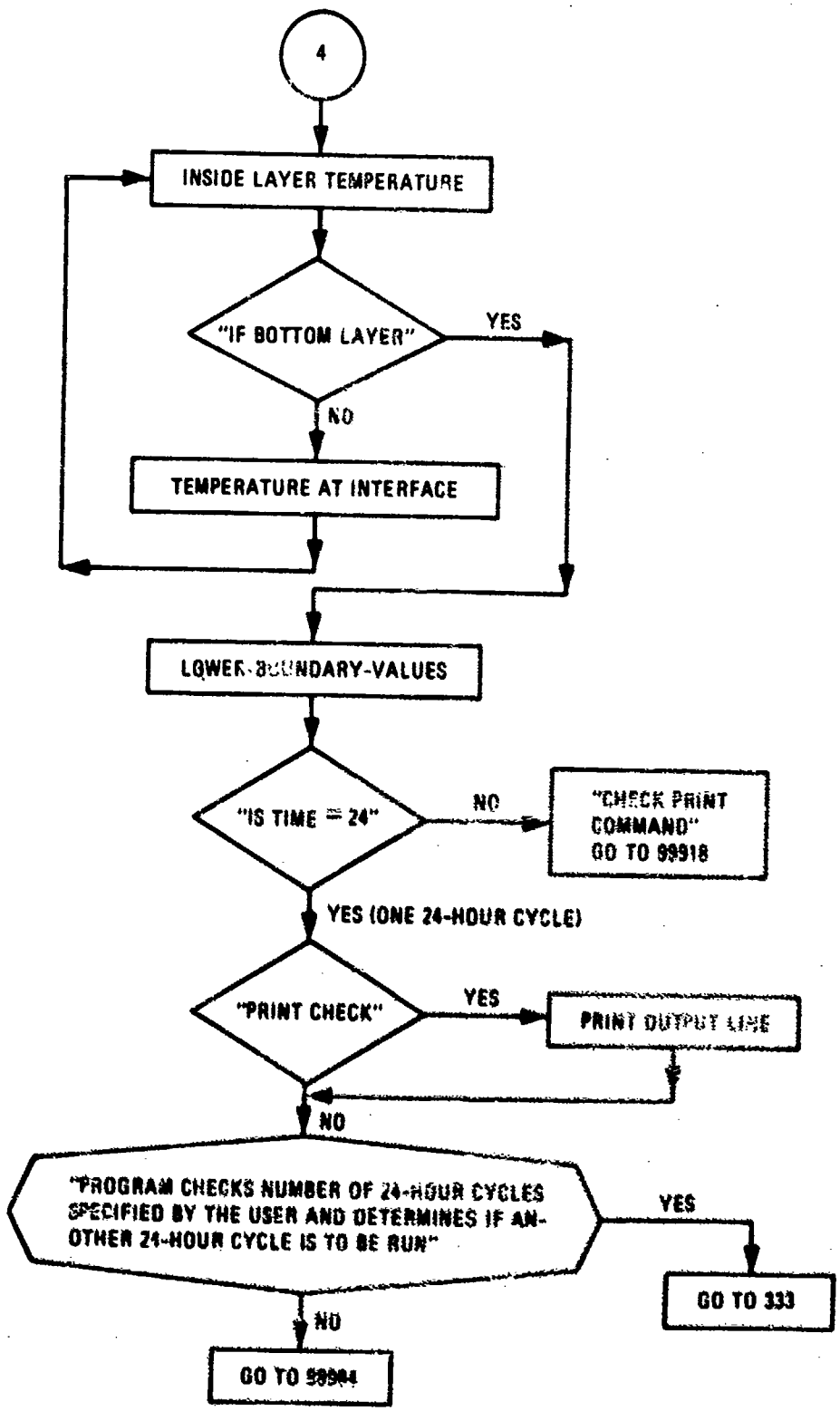

Figure A1. (Sheet 5 of 5)

Table A1

Variable Definitions

Variable	Definition
ALPH(IX)	THERMAL DIFFUSIVITY OF LAYER IX IN CM**2/MIN
APRM	FACTE*TEMP**3 IN CAL/MIN**2-CM**2
ATERM	ENERGY CONTRIBUTED BY ATMOSPHERIC IR EMISSION CAL/CM**2-MIN
B	HEAT CONDUCTIVITY OF SURFACE CAL/CM**2-MIN-K
BBB(J,I)	Y INTERCEPT OF LINEAR EQUATION, USED FOR TABLE INTERPOLATION
BEP	BOTTOM SURFACE EMISSIVITY
BK	BOTTOM SURFACE GEOMETRIC SHAPE IN FRACTION (0.0-1.0)
BPRM	HEAT CONDUCTIVITY OF BOTTOM BOUNDARY LAYER
BTERM	ENERGY CONTRIBUTED BY INSOLATION AFTER ADJUSTMENT USING SURFACE ABSORPTIVITY. IN CAL/CM**2-MIN
CLOUD	CLOUD COVER IN FRACTION OF 0.1-1.0
DAY	JULIAN DAY USED IN SOLVING INSOLATION
DECL	SOLAR DECLINATION ANGLE
DELT	TIME STEP IN HOURS
DIST	DEPTH IN CM OF INITIAL SOIL PROFILE AT WHICH CORRESPONDING SOIL TEMPERATURE IN KELVIN IS INTERPOLATED
DPRM	HEAT FLUX IN CAL/CM**2-MIN BOTTOM BOUNDARY OR TEMPERATURE IN KELVIN AT BOTTOM BOUNDARY
DPRMO	TEMPERATURE OF BOTTOM MATERIAL IN DEGREE CELSIUS. USED WHEN LFLUXY = 0
DPRM1	HEAT FLUX THROUGH BOTTOM MATERIAL, IN CAL/CM**2-MIN, USED WHEN LFLUXY NOT EQUAL 0
DTERM	ENERGY LOSS DUE TO EVAPORATION
ELF	LATITUDE IN RADIANS
EPSN	EMISSIVITY OF SURFACE MATERIAL
FACTA	SIGMA*EPSN
FACTD	FACTD=SIGMA*BK*BEP*TR**4 USED IN BOTTOM BOUNDARY CALCULATION WHEN THERE IS AIR SPACE BENEATH THE BOTTOM
FACTE	FACTE=SIGMA*BK*BEP

(Continued)

Table A1 (Continued)

Variable	Definition
FACTH	USED IN SOLVING CONVECTION TERM (HTERM) (1000.0/PRESS)** 0.286
FK(IX)	HEAT CONDUCTIVITY OF LAYER IX IN CAL/MIN-CM-K
FMM(J,I)	SLOPE OF LINEAR EQUATION, USED FOR TABLE INTERPOLATION OF HOURLY INPUT DATA
HEADER	72 CHARACTER INPUT VARIABLE USED TO PRINT COMMENTS ON OUTPUT
HTERM	ENERGY LOSS OR GAIN DUE TO CONVECTION CAL/CM**2-MIN
IEFSWT	SWITCH WHEN = 0 WILL PRINT OUTPUT ONLY AT SPECIFIED TIME. IF NOT = 0 WILL PRINT OUTPUT AT EVERY ITERATION
IEOF	SET FROM 0 TO 1 WHEN IEOF IS ENCOUNTERED, USED TO TERMINATE PROGRAM
IMATL	BACKWARD COUNTER OF LAYERS. STARTING WITH THE NUMBER OF LAYERS
INTR(IX)	BEGINNING SUB-LAYER DEPTH NUMBER FOR LAYER NUMBER IX
IPRNT	BACKWARD COUNTER SET=NPRNT. WHEN EQUAL TO 1 OUTPUT IS PRINTED
ITIME	BACKWARD COUNTER INITIALIZED AS TOTAL TIME STEPS IN HOURS
IX	LAYER NUMBER STARTING WITH TOP LAYER
IY	SUB-LAYER DEPTH NUMBER
JMAX	THE TOTAL NUMBER OF SUB-LAYERS
LAT	LATITUDE USED IN SOLVING INSOLATION
LFLUXY	INPUT BOTTOM BOUNDARY DATA CONTROL SWITCH. IF = 0, THERE IS NO HEAT FLUX THROUGH BOTTOM OF MATERIAL, IF NEGATIVE THERE IS NO AIR SPACE BENEATH BOTTOM MATERIAL, IF POSITIVE THERE IS AIR SPACE BENEATH BOTTOM MATERIAL
L1	DUMMY VARIABLE TO READ LINE NUMBER FROM INPUT FILE
M	SECANT OF SOLAR ZENITH ANGLE IN RADIANS
MAX(J)	NUMBER OF INPUT TABLE VALUES USED IN TABLE INTERPOLATION MODULE
NCLOUD	CLOUD TYPE INDEX NUMBER (1-8) USED IN SOLVING INSOLATION, INFRARED EMISSION
NOMATL	NUMBER OF MATERIAL LAYERS USED IN SOLVING HEAT FLOW
NPRNT	NUMBER OF TIMES OUTPUT TIME PRINT FREQUENCY IS DIVISIBLE BY TIME STEPS. USED TO DETERMINE WHEN TO PRINT OUTPUT

(Continued)

Table A1 (Continued)

Variable	Definition
NTABL	TABLE NUMBER
NX(IX)	NUMBER OF SUBLAYER OF EACH LAYER, NX(IX) = THK(IX)/ SFRQ(IX)
PRESS	ATMOSPHERIC PRESSURE IN MILLIBAR(MB) USED IN SOLVING INSOLATION
PTYME	BEGINNING TIME OF OUTPUT=TOTAL NUMBER OF HOURS MINUS 24 USED IN PRINT-OUTPUT MODULE 2
REP	EMISSIVITY BENEATH AIR SPACE
RHOC(IX)	FK(IX)/ALPH(IX) IN CAL/CM**2-K
RI	RICHARDSON INDEX NUMBER USE IN SOLVING CONVECTION ENERGY LOSS
RK	SURFACE BENEATH AIR SPACE GEOMETRIC SHAPE IN FRACTION (0.0-1.0)
RR(IX)	RR(IX)=DELT/SFRQ**2. (PART OF HEAT FLOW EQUATION)
SAZ	SOLAR AZIMUTH IN RADIANS, SAZ=ATAN (-COS(DECL)*SIN(TIMER)/ (COS(ELF*SIN(DECL)-SIN(ELF)*COS(TIMER))))
SFRQ(IX)	VERTICAL GRID SPACING IN CM IN EACH LAYER IX IN CM**2/MIN
SICF	INSOLATION ADJUSTMENT DUE TO ZENITH ANGLE, SURFACE SLOPE AND SURFACE ASPECT ANGLE, SICF=COS(Z)*COS(SLOPE)*SIN(Z)*
SLOPE	SURFACE SLOPE IN DEGREES WITH HORIZONTAL=0 DEGREE, USED IN SOLVING INSOLATION
SMALLA	ABSORPTIVITY OF SURFACE MATERIAL
SOLCHX	EQUALS SOLAR INSOLATION AT 1200 HOURS, USED TO DETERMINE IF SOLAR INSOLATION IS INPUT
SPEED	WING SPEED IN CM/SEC
STOR(1,IY)	ESTIMATE SUB-LAYER TEMPERATURE IN KELVIN
STOR(2,IY)	FK: HEAT CONDUCTIVITY OF SUB-LAYER IY IN CAL/MIN-CM-K
STOR(3,IY)	RHOC, FK/ALPH IN CAL/CM**2-K
STOR(4,IY)	CONSTANT DIMENSIONLESS
STOR(5,IY)	INITIAL SOIL TEMPERATURE IN KELVIN OF INITIAL SOIL PROFILE
STOR(6,IY)	SAME AS STOR(2,IY)
STOR(7,IY)	SAME AS STOR(3,IY)

(Continued)

Table A1 (Continued)

Variable	Definition
SUN	CALCULATED INSOLATION VALUE
SURFACAZ	SURFACE AZIMUTH IN DEGREE WITH SOUTH = 0 DEGREE, USED IN SOLVING INSOLATION
T	SAME AS TIME
TA	AIR TEMPERATURE IN KELVIN
TAC	AIR TEMPERATURE IN DEGREE CELSIUS
TAK	AIR TEMPERATURE IN KELVIN
TB	THERMAL CONDUCTIVITY OF BOTTOM MATERIAL CAL/CM**2-DEG C-MIN
TFREQ	TIME STEP IN MINUTES USED IN SOLVING HEAT FLOW
THK(IX)	LAYER THICKNESS IN CM OF LAYER IX
TIME	TIME IN HOURS IN WHICH MATERIAL TEMPERATURES ARE ESTIMATED
TIMER	SUN'S HOUR ANGLE IN RADIANS
TOTTIM	TOTAL NUMBER OF 24 HOUR REPETITIONS USED IN SOLVING HEAT FLOW
TPRNT	OUTPUT TIME PRINT FREQUENCY IN MINUTES
TR	TEMPERATURE OF AIR SPACE BENEATH BOTTOM MATERIAL
TSK	MATERIAL SUB-LAYER TEMPERATURE IN KELVIN
TYME	TIME IN HOURS USE INSOLATION CALCULATION
WATER	THE AMOUNT OF PRECIPITAL WATER IN MILLIMETRES (MM) CALCULATED FOR USE IN SOLVING INSOLATION
WET	MOISTURE CONTENT OF SURFACE MATERIAL
XL	LATENT HEAT OF EVAPORATION AS FUNCTION OF AIR AND GROUND TEMPERATURE
XXX(J,1)	TIME IN HOURS (AIR TEMPERATURE)
XXX(J,2)	TIME IN HOURS (RELATIVE HUMIDITY)
XXX(J,6)	TIME IN HOURS (WIND SPEED)
XXX(J,3)	TIME IN HOURS (AMOUNT OF CLOUD COVER)
XXX(J,4)	TIME IN HOURS
XXX(J,5)	DEPTH IN CENTIMETRES OF POINTS IN INITIAL TEMPERATURE PROFILE

(Continued)

Table A1 (Concluded)

Variable	Definition
YYY(J,1)	AIR TEMPERATURE IN DEGREES CELSIUS TABLE 1
YYY(J,2)	RELATIVE HUMIDITY INPUT FRACTION, USED IN TABLE 2 SOLVING INFRARED EMISSIONS, (ATERM) EVAPORATIVE HEAT LOSS (DTERM)
YYY(J,6)	WIND SPEED INPUT IN METRES/SECOND AND CONVERTED TO CENTIMETRE/SECOND TABLE 6
YYY(J,3)	AMOUNT OF CLOUD COVER IN FRACTION (0 TO 1) USED IN SOLVING INSOLATION TABLE 3 INFRARED EMISSION (ATERM)
YYY(J,4)	INSOLATION IN CAL/CM**2-MIN, IF 0.0 AT 12000 HOURS, INSOLATION VALUES WILL CALCULATE TABLE 4
YYY(J,5)	TEMPERATURE IN DEGREES CELSIUS AT POINTS IN INITIAL TEMPERATURE PROFILE
Z	SOLAR ZENITH ANGLE, Z=SIN(DECL)*SIN(ELF)+COS(DECL)* COX(ELF)*COS(TIMER)
ZA	SHELTER HEIGHT IN CENTIMETRES (CM)
ZZA	SURFACE TEMPERATURE OF MATERIAL IN KELVIN
ZZB	BOTTOM LAYER TEMPERATURE OF MATERIAL IN KELVIN

APPENDIX B: TYPICAL VALUES FOR SYSTEM DESCRIPTORS

Table B1

Representative Input Parameters for Some Common Materials*

Substance	Shortwave Absorptivity	Longwave Emissivity	Thermal Conductivity $cal/cm^2\text{-}min\text{-}^\circ K$	Thermal Diffusivity cm^2/min
		Natural Materials		
Sandy soil				
Frozen	0.57-0.66	0.91-0.93	0.09	0.36
Unfrozen	--	--	0.08	0.30
Clayey soil				
Frozen	0.4	0.88-0.97	0.13	0.39
Unfrozen	--	--	0.11	0.26
Top soil				
Fallow	0.88-0.95	0.8	0.20	0.310
Ploughed field	0.86-0.9	--	--	--
Sandy gravel	0.28	0.28	0.347	0.48
Granite	0.55-0.65	0.89	0.496	0.96
Limestone	0.7-0.8	0.9	0.13	0.29
Sandstone, quartz	0.3-0.4	0.94	0.37-0.72	0.78
Fresh snow	0.05-0.25	0.12	0.03	0.06
Old snow				
Clean	0.35-0.50	0.98	0.08	0.24
Dirty	0.50-0.80	0.98	--	--
Ice	0.31	0.63-0.90	0.31	0.70
Forest duff	0.92-0.95	0.7	0.010	0.74
		Construction Materials		
Concrete (dry)				
Aerated	0.7	0.94-0.97	0.011	0.17
Dense	--	--	0.22	0.43
Brick				
Red Masonry	0.55-0.7	0.9	0.074-0.12	0.21-0.35
Fireclay (medium brown)	0.27	0.75	0.14	0.41
Lumber				
Hardwood	0.6	0.90	0.03	0.07
Softwood	--	--	0.012-0.022	0.11
Tarpaper	0.95	0.93	--	--
Asbestos sheets	0.8	0.96	0.017	0.09
Asphalt	0.8-0.95	0.96	0.10	0.22
Stainless steel	0.5	0.12	3.0	3.2
White plaster	0.07	0.91	0.11	0.2
Galvanized iron				
Bright	0.63	0.13	--	--
Oxidized gray	0.8	0.28	--	--
Cast iron	0.45	0.44	6.8	7.9
Wrought iron	--	--	8.6	9.3
Glass	--	0.84-0.94	0.15-0.20	0.18-0.75
Polystyrene	--	--	0.004	0.9
Aluminum	0.15	0.04-0.09	32.0	5.4
		Surface Coatings		
Solid $MgCO_3$	0.04	0.79	--	--
White CaO	0.15	0.96	--	--
Gray CaO	0.97	0.87	--	--
White paint (0.04 cm on Al)	0.2	0.91	--	--
Black paint (0.04 cm on Al)	0.96	0.88	--	--
Aluminum paint	0.2	0.4	--	--
Clear varnish on Al	0.8	0.2	--	--
Rust	0.94	0.80-0.94	--	--

* Link 1979; Oke 1978; Wechsler and Glaser 1966; Buettner and Kern 1965; Jumikis 1977; American Society of Heating, Refrigerating, and Air-Conditioning Engineers 1977; and personal communication, G. Pech, Petawawa National Forestry Institute, Canadian Forestry Service, Chalk River, Ontario, Canada.

In accordance with letter from DAEN-RDC, DAEN-ASI dated 22 July 1977, Subject: Facsimile Catalog Cards for Laboratory Technical Publications, a facsimile catalog card in Library of Congress MARC format is reproduced below.

Thermal modeling of terrain surface elements : final report / by L. K. Balick (Lee K.) ... [et al.] (Environmental Laboratory, U.S. Army Engineer Waterways Experiment Station) ; prepared for Headquarters, Department of the Army. -- Vicksburg, Miss. : U.S. Army Engineer Waterways Experiment Station ; Springfield, Va. : available from NTIS, 1981.
42, [43] p. : ill. ; 27 cm. -- (Technical report / U.S. Army Engineer Waterways Experiment Station ; EL-81-2)
Cover title.
"March 1981."
"Under Project No. 4762730AT42, Task A4, Work Unit 003 and 4762719AT40, Task CO, Work Unit 006."
Bibliography: p. 41-42.

1. Infrared technology. 2. Mathematical models. 3. Military reconnaissance. 4. Relief models. 5. Temperature. I. Balick, L. K. (Lee K.) II. United States. Dept. of the Army. III. United States. Army

Thermal modeling of terrain surface elements : ... 1981.
(Card 2)

Engineer Waterways Experiment Station. Environmental Laboratory. IV. Title V. Series: Technical report (United States. Army Engineer Waterways Experiment Station) ; EL-81-2.
TA7.W34 no.EL-81-2